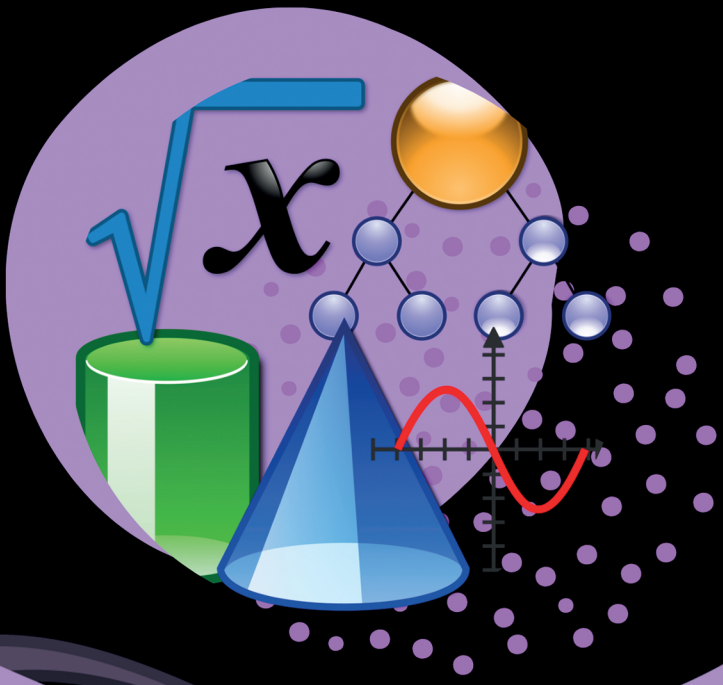
DOI: 10.5281/zenodo.7744418

INTERNATIONAL RESEARCH IN SCIENCE AND MATHEMATICS



EDITOR
Prof. Rıdvan KARAPINAR,Ph.D.

Platanus Publishing®

INTERNATIONAL RESEARCH IN SCIENCE AND MATHEMATICS

EDITOR
Prof. Rıdvan KARAPINAR, Ph.D.

İmtiyaz Sahibi
Platanus Publishing®

Editor
Prof. Dursun KOSE, Ph.D.

Kapak & Mizanpaj & Sosyal Medya

Platanus Yayın Grubu

Birinci Basım
Mart, 2023

Yayımcı Sertifika No
45813

Matbaa Sertifika No
47381

ISBN
978-625-6971-51-6

© copyright
Bu kitabın yayım hakkı Platanus Publishing'e aittir.
Kaynak gösterilmeden alıntı yapılamaz, izin
alınmadan hiçbir yolla çoğaltılamaz.

Platanus Publishing®
Adres: Natoyolu Cad. Fahri Korutürk Mah. 157/B,
06480, Mamak, Ankara, Türkiye.
Telefon: +90 312 390 1 118
web: www.platanuskitap.com
e-mail: platanuskitap@gmail.com



PLATANUS PUBLISHING®

CONTENTS

CHAPTER 1 ..... **5**

Morphological Analysis of Si-Doped Czts Thin Films By Sem and Afm

Arş. Gör. Canan AYTUĞ AVA

Prof Sezai ASUBAY, Ph.D

CHAPTER 2 ..... **17**

A New Approach to Superposition Operators on Some Non-Newtonian Maddox Sequence Spaces

Dr. Fatmanur ERDOĞAN

Prof. Birsen SAĞIR, Ph.D

CHAPTER 3 ..... **31**

Cydonia Oblonga Mill.: The Evaluation of the Leaves For Biologial and Coloring Properties as A Sustainable Fabric Dye

Prof. Tülin AŞKUN, Ph.D.

Ph.D. Student Pınar GÜNER

Prof. Gülendam TÜMEN, Ph.D.

Prof. Fatih SATIL Ph.D.

CHAPTER 4 ..... **53**

Glutathione (Gsh-Gssg)

Assistant Professor Ebru COTELI

CHAPTER 5 ..... **63**

Manipulatıon of Gut Microbiota Bacterıa For Therapeutic Purposes

Assist. Prof. Taha CEYLANI, Ph.D

CHAPTER 6 ..... **79**

First TESS Light Curve Solution of V458 And

Research Asst. Oğuz ÖZTÜRK, PhD


CHAPTER
1

ISBN: 978-625-6971-51-6

MORPHOLOGICAL ANALYSIS OF SI-DOPED CZTS THIN FILMS BY SEM AND AFM

Arş. Gör. Canan AYTUĞ AVA
Dicle Üniversitesi Fen Bilimleri Enstitüsü
ORCID: 0000-0003-4771-816X

Prof Sezai ASUBAY, Ph.D
Dicle Üniversitesi Fen Fakültesi
ORCID: 0000-0003-2171-8479

1. INTRODUCTION

When we look at the history of human culture, it is seen that the search for energy has come since existence. With the discovery of fire, the energy obtained by the combustion reaction of wood was used as a heat source in heating and meeting many energy needs such as cooking. Later, in modern times, James Watt's steam engines played an important role in industrialization, converting fossil fuels such as coal, natural energies, into usable energies. The ability to transform existing energy into usable energy has helped human beings become richer both economically and scientifically and lead a more luxurious life (Yıldırım., 2022). Today, energy has become necessary for many basic needs of humanity, from transportation to lighting, from communication to feeding and heating. The fossil fuels used in this transformation are still used as a primary energy source in today's world. However, the trend of depletion of fossil fuels is increasing day by day. While the reduction of these resources is a major energy problem in the world, the CO gas released during the conversion of these resources into usable energy also triggers environmental pollution and global warming.

According to the data of the National Energy Agency (IEA), coal demand experienced the biggest decrease with a decrease of 4% since World War II, with the measures taken during the Covid-19 period . (İEA, 2021) However, in 2021, it is expected that as the economy recovers, it will reverse the decline in coal demand in 2020 and exceed coal demand in 2019 with an increase of 4.5% (İEA,

2021). Likewise, due to the increasing shortage of natural gas and coal in crude oil, oil prices have been scaled to the highest levels of several years.

The common view of all these researches is to increase the use of renewable energy sources and to develop these technologies. In this year's report on renewable electricity by the IEA, global renewable electricity capacity is expected to reach over 4,800 GW by 2026, an increase of over 60% from 2020 levels. The capacity is equivalent to the combined available total global power capacity of fossil fuels and nuclear power. Renewable energy is expected to account for almost 95% of the increase in global power capacity by 2026, with photovoltaic (PV) cells alone providing more than half. The amount of renewable capacity added in the period 2021 to 2026 is expected to be 50% higher than between 2015 and 2020. This is due to stronger support from the policies of governments supporting renewable energy and the more ambitious clean energy targets announced before and during the COP26 Climate Change Conference (İEA, 2021).

Solar energy stands out among renewable energy sources due to its features such as being accessible all over the world, being clean and sustainable. The solar energy falling on the world is about 36 x 1017 kWh, and the current world consumption is about 0.5 x 1014 kWh per year (Muratoglu and Yuce, 2015). PV cells have been invented to convert some of this energy from the sun to a usable energy source such as electricity. Today, 90% of the PV cell market consists of Si-based PV cells, while the remaining 10% is thin-film PV cells. The biggest disadvantage of Si-based solar cells is their high cost, low optical absorption coefficient (<104 cm1) depending on their thickness, and the use of more than one hundred materials (Poortmans and Arkhipov, 2006). For this reason, scientists are trying to produce more energy and increase the efficiency value by using less material by using thin-film solar cells. When looking at the thin-film solar cells that are commercially available today, it is seen that the maximum efficiency values obtained in CdTe, Cu(In,Ga)Se2 (ClGSe) and amorphous Si-based solar cells are over 20% (Jackson et al. 2016), (https://www.greentechmedia.com), (Nakamura et al., 2019). With the CIGS solar cell, the world record in the laboratory environment was increased to 29.1% (Solar cell efficiency,Martin A. Green) However, In (Indium), Ga (Gallium) and Te (Tellurea) in the structure of CIGS and CdTe are rare elements in the earth's crust and Cd (Cadmium) is toxic elements.

The CZTS quaternary compound semiconductor has recently been considered as an alternative to CIGS absorber layers, due to its favorable optical absorption coefficient ($>10^4$ cm^1), ideal band gap (1.5 eV), and non-toxic elements that are abundant in the earth's crust. (Wolden et al.,2011), (Wang et al. 2021). Although

ISBN: 978-625-6971-51-6

there have been intense studies on CZTS and CZTSSe-based thin-film solar cells in recent years, it is seen that the efficiency values are far below the theoretical limit value and there is still a big performance difference between CZTS-based CIGS-based solar cells. This is thought to be largely due to the fact that CZTS-based cells have a larger open-circuit voltage gap (Giraldo et al.,2019). In cases where the necessary pressure and temperature range for CZTS formation is not established, many side phases (SnS, ZnS, CuS, CTS, etc.) occur.

Atomic force microscopy (AFM) is one of the most important tools used to explore materials at the scale of a few nanometers, a technique used for surface characterization. It gives surface images without any chemical etching or staining. The unique feature of this technique compared to other microscopy techniques is that we can examine its mechanical properties and it does not involve the use of surface-damaging electron beam radiation.

A scanning electron microscope (SEM) is a type of electron microscope that obtains images by scanning the sample surface with a focused beam of electrons. Electrons interact with atoms in the sample to produce different signals that contain information about the topography and composition on the sample surface. These signals are collected by the relevant detectors and transferred to the computer screen and an image is obtained.

The presence of EDS capability with the SEM device is crucial for the qualitative and quantitative analysis of any sample. In the absence of EDS, only information about the surface topography of the sample can be generated via SEM. The two most powerful features of SEM imaging are secondary electron imaging and backscattered electron imaging. Understanding the working principle of both features is essential to have a complete understanding of how the SEM device works. SEM is characterized by its easy use. The person who has this knowledge can be able to perform the analysis and get smooth imaging.

In this study, the surface morphology of the film obtained by substituting Si instead of Sn in CZTS thin films was examined by atomic force microscope and scanning electron microscope.

2. MATERIALS AND METHOD

The coating process is carried out using pre-cleaned glass substrates with dimensions of 26×76 mm. In order to prepare a semiconductor that is close to ideal, it is recommended to clean the semiconductor very well chemically. In the case of a good cleaning process, many surface defects that may occur in the semiconductor will be eliminated. All chemical cleaning and rinsing processes of the semiconductor are carried out in an ultrasonic bath in order to clean the dirt on the crystal surface and remove the roughness on the surface. In this study, the cleaning of glass substrates was carried out by applying the RCA procedure.

In this study, CZTS:Si thin films were deposited on glass surfaces by spin coating method, then annealed and characterized under 40 ccm H_2S: Ar (1:9) flow. As Cu, Zn, Sn and Si sources, 0.08 M Copper chloride (CuCl2), 0.04 M Zinc chloride (ZnCl2), 0.04 M tin (II) chloride dihydrate (SnCl2.H2O), 0.04 M Silicon isopropoxide solutions were used. During the preparation of the solutions, after adding ZnCl2 solution to the CuCl2 solution, sufficient amount of Silicon isopropoxide was added to the CuCl2/ZnCl2 solution and finally $SnCl2.H_2O$ was added. 0.1 ml of diethanolamine was added to the mixing solution and the solutions were stirred for 3 hours. 0.5 ml of the mixing solution was dropped on the glass substrates, then the glasses were rotated at 5000 rpm for 30 seconds and then heated at 240°C for 10 minutes to form compact thin films. After repeating these processes 10 times Cu_2Zn(Si:Sn) thin films were annealed in a high temperature (550 °C) quartz furnace in H2S environment in 40 ccm H_2S:Ar (1:9) flow for 2 hours. With this method, CZSiS thin films annealed under 40 ccm H_2S:Ar (1:9) fluxes were obtained. (Aytuğ Ava et al., 2022)

3. FIGURES AND TABLES

The AFM and SEM images of the thin films obtained by annealing Cu_2ZnSn:SiS_4 films, which were deposited in 40 ccm Ar:H_2S medium and at different concentrations (0%, 50%, 100%) under H_2S fluxes, at 550 °C for 2 hours are given. Films with 0% Si contribution in this study CZTS, films with 50% Si contribution were named CZSn:SiS and films with 100% Si contribution were called CZSiS. In line with the information obtained from the figures and tables we examined, the Ra, Rq and Rz values of 2D and 3D AFM images of doped CZTS thin films were examined. This values given in AFM analysis:

Ra: Arithmetic mean of surface roughness

Rq: Geometric mean of profile irregularities

Rz: Average roughness depth

ISBN: 978-625-6971-51-6

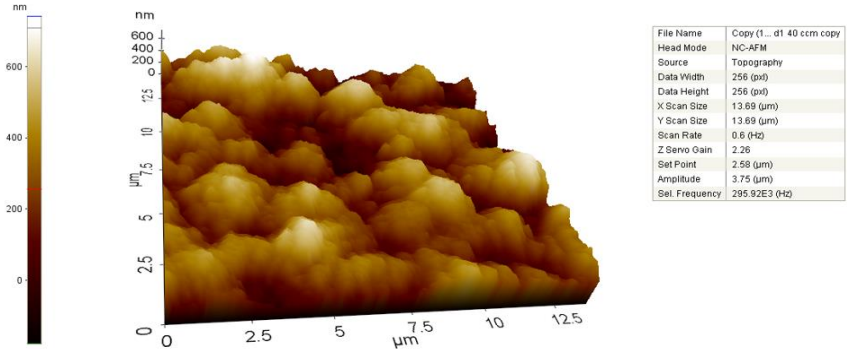


Figure 1. AFM image of CZSnS thin film 3D

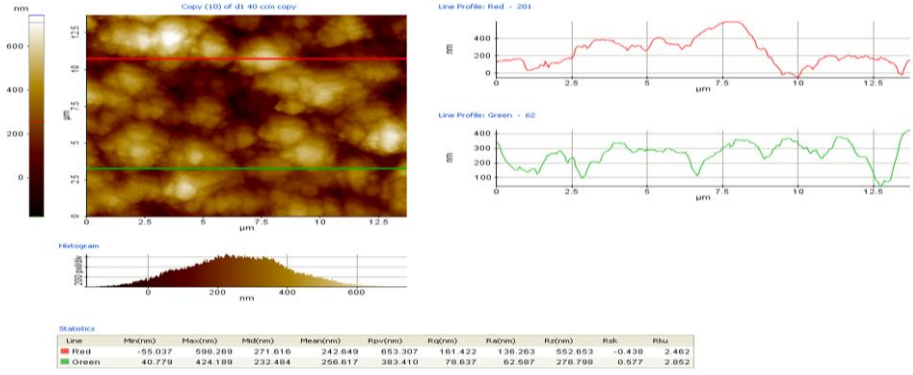


Figure 2. AFM image of CZSnS thin film 2D

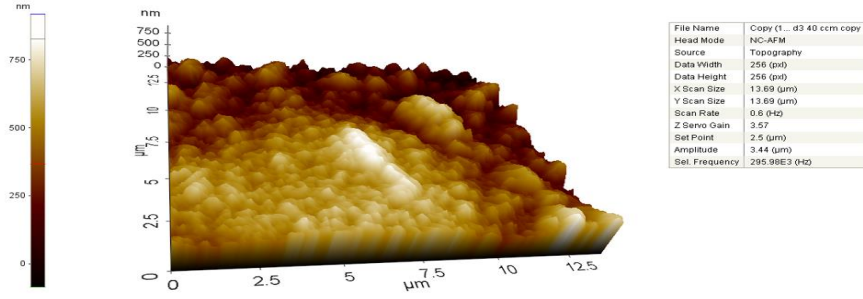


Figure 3. AFM image of CZSn:SiS thin film 3D

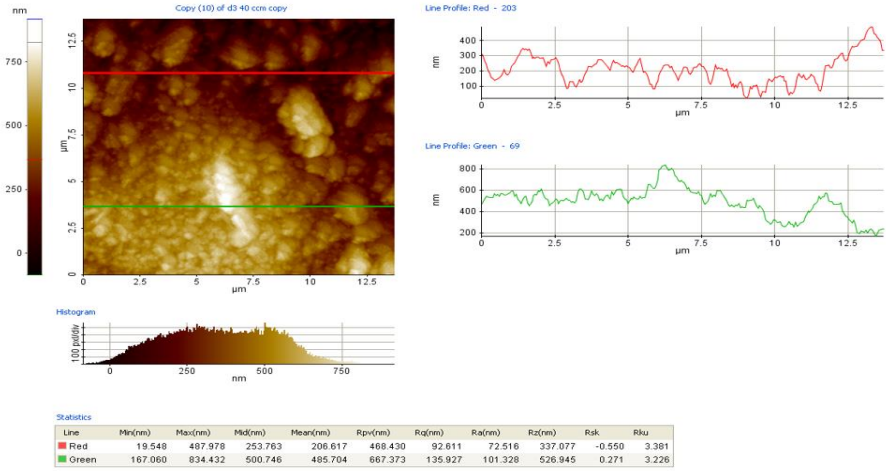


Figure 4. AFM image of CZSn:SiS thin film 2D

ISBN: 978-625-6971-51-6

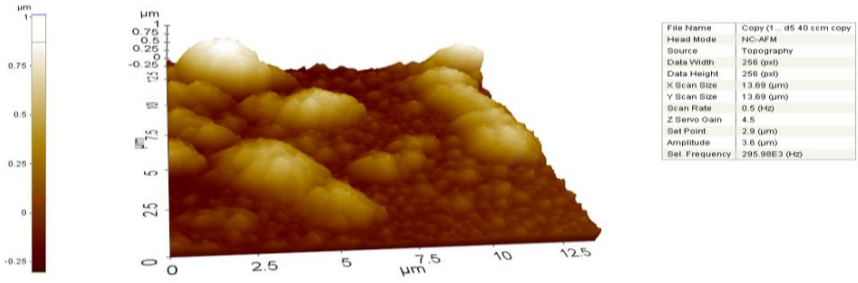


Figure 5. AFM image of CZSiS thin film 3D

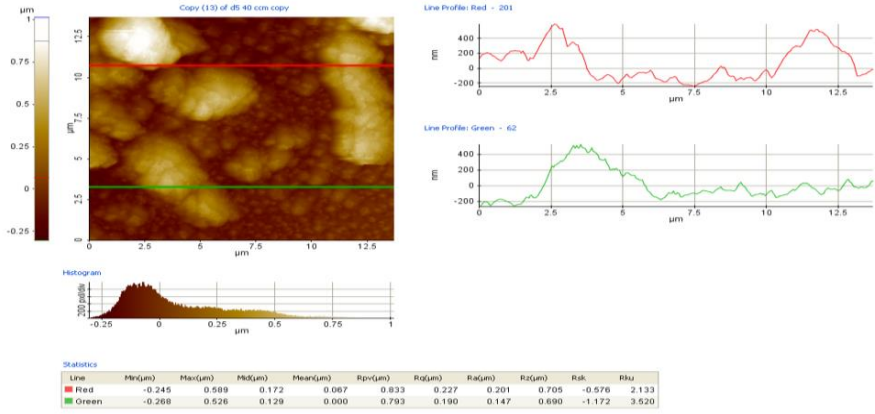


Figure 6. AFM image of CZSiS thin film 2D

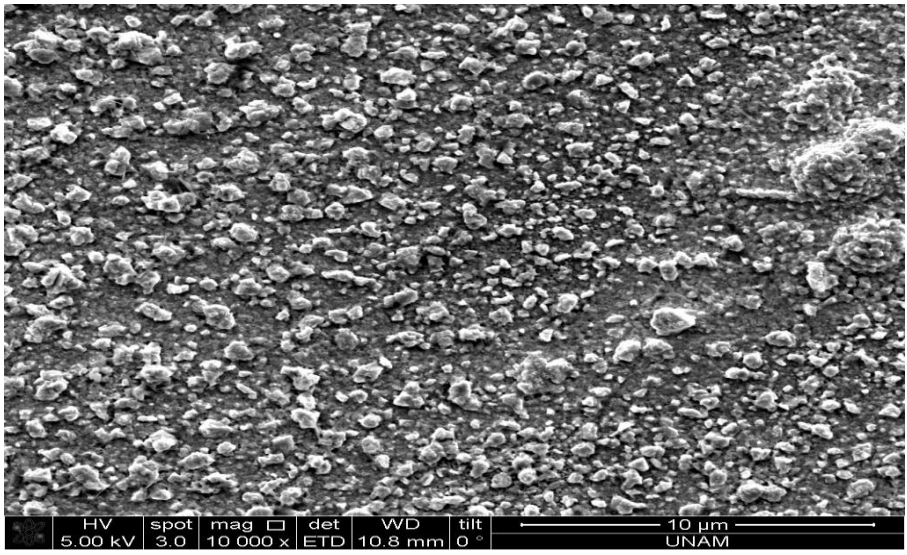


Figure 7. SEM image of CZSnS thin film

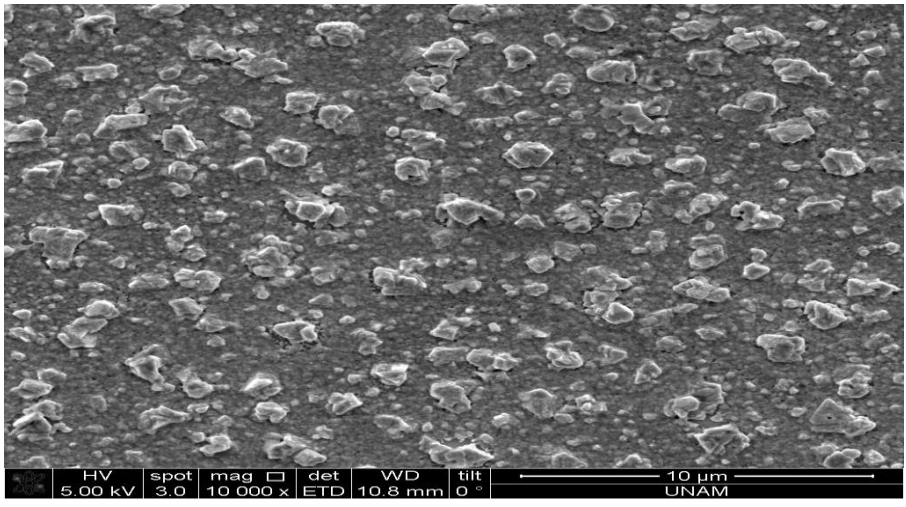


Figure 8. SEM image of CZSn:SiS thin film

ISBN: 978-625-6971-51-6

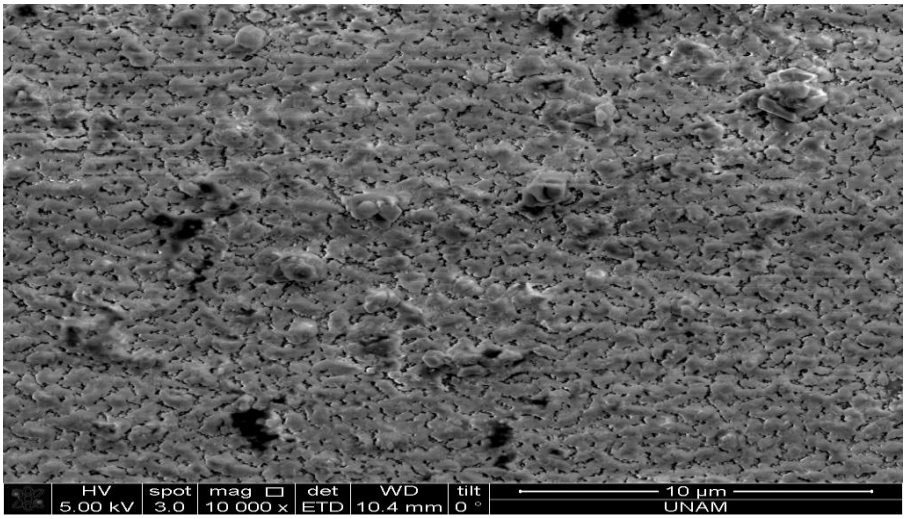


Figure 9. SEM image of CZSiS thin film

4.RESULTS

The surface roughness of doped and undoped CZTS thin films is not uniform and homogeneous. As can be seen from the values given in the table, it was observed that the particle size of the CZSn:SiS thin film annealed under 40 cc H2S gas was very small and the surface was more homogeneous. Looking at the 3D AFM image of the CZSn:SiS thin film, it was seen that the height of the surface profile was 250 nm and it was smaller compared to other films. As si was added, there was a very rapid decrease in values. As the amount of additive increased, very small surface roughness was observed on the surface of the doped material. As doping increased, particle size and roughness decreased. As a result, the additive showed a reduction of approximately 700% on the material. The lowest numerical values of the roughness depth, the average roughness value and the geometric mean of the profile irregularities were seen in the 100% doped film.

When the sections taken during the surface analysis and Ra, Rq and Rz values are examined in detail; It has been observed that the surfaces of CZTS films generally have a homogeneous distribution in the sections taken. CZSiS films create a more homogeneous surface profile. It was observed that the CZTS films showed a rougher distribution and the particle size was larger when the additive ratio decreased. When the SEM images obtained were examined, it was observed that they matched exactly with the AFM images.

Table 1: Ra, Rq and Rz values of AFM parameters

Sample	Surface Roughness (nm)		
	R_a	R_q	Rz
CZSnS	136.6/62.5	161.4/78.6	552.6/278.8
CZSn:SiS	72.5/101.3	92.6/135.9	337/506.9
CZSiS	0.2/0.14	0.22/0.19	0.7/0.69

5. CONCLUSION

As a result of the studies, AFM images of doped and undoped thin films were taken. Surface roughness values, average roughness values and profile roughness were examined. The results are stated in the table. The results of the SEM analysis and AFM analysis overlap with each other. It was observed that the surface profile changed as a result of the additives.

ACKNOWLEDGMENT

I would like to thank Assoc. Prof. Yusuf Selim OCAK and Assoc. Prof. Ömer ÇELIK for their contributions.

I would like to thank Dicle University Science and Technology Application and Research center (DUBTAM) for its contributions.

ISBN: 978-625-6971-51-6

REFERENCES

A. Muratoglu, M.I. Yuce, World energy outlook and place of renewable resources,

Int. J. Sci. and Tech. Rech. 1/10–17 https://www.researchgate.net/ (2015).

Ao Wang et al. 'Analysis of manufacturing cost and market niches for Cu2ZnSnS4 (CZTS) solar cells' Sustainable Energy Fuels, (2021)

Aytuğ Ava C., Ocak. Y.S., Celik. O., Asubay .S. (2022) Deposition and Characterization of Si Substituted Cu2ZnSnS4 Thin Films. *Silicon.* https://doi.org/10.1007/s12633-022-02018-6

Fotovoltaik Uygulamalar için CZTS (Cu_2SnZnS_4) İnce Filmlerin Sentezi ve Karakterizasyonu Ali Rıza Yıldırım Yüksek Lisans Tezi. Hacettepe/Ankara. (2022).

https://www.greentechmedia.com/articles/read/First-Solar-Hits-Record-22-1-Conversion-Efficiency-For-CdTe-Solar-Cell

İEA, Oil Market Report, 2021 https://www.iea.org/reports/oil-market-report-october-(2021)

İEA, Renewable electricity growth is accelerating faster than ever worldwide, supporting the emergence of the new global energy economy. 2021. https://www.iea.org/news/renewable-electricity-growth-is-accelerating-faster-than-ever-worldwide-supporting-the-emergence-of-the-new-global-energy-economy

Jef Poortmans, Vladimir Arkhipov. 'Thin Film Solar Cells: Fabrication, Characterization and Applications'. (2006)

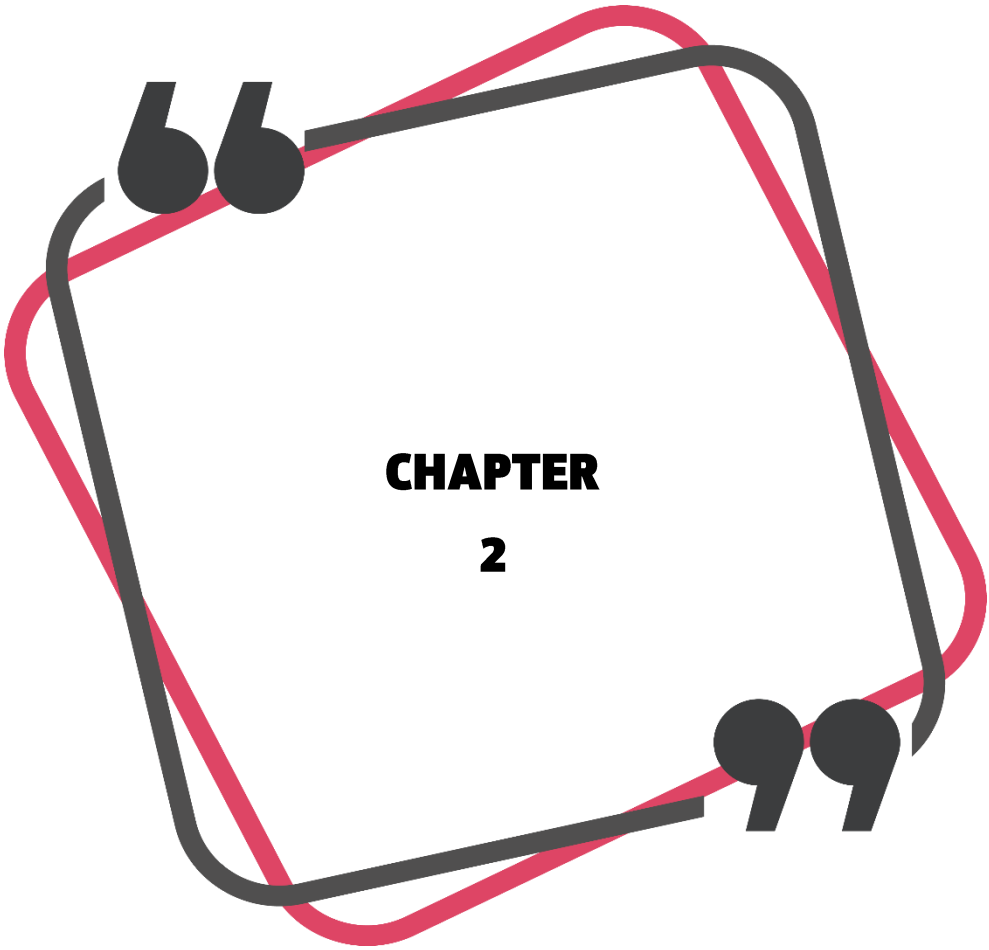
Motoshi Nakamura, Koji Yamaguchi, Yoshinori Kimoto et al. 'Cd-Free Cu(In,Ga)(Se,S)2 Thin-Film Solar Cell With Record Efficiency of 23.35%.' IEEE JOURNAL OF PHOTOVOLTAICS. 10.1109/JPHOTOV.2019.2937218. (2019).

P. Jackson, R. Wuerz, D. Hariskos, E. Lotter, W. Witte, M. Powalla, 'Effects of heavy alkali elements in Cu(In,Ga)Se2 solar cells with efficiencies up to 22.6%.' Phys. Status Solidi RRL 10 (2016).

Sergio Giraldo et al. 'Progress and Perspectives of Thin Film Kesterite Photovoltaic Technology: A Critical Review.' Adv. Mater. (2019)

Solar cell efficiency tables (version 59) Martin A. Green.

Wolden, C.A., Kurtin, J., Baxter, J.B., Repins, I., Shaheen, S.E., Torvik, J.T., Rockett, A.A., Fthenakis, V.M., Aydil, E.S., 'Photovoltaic manufacturing: present status, future prospects, and research needs.' J. Vac. Sci. Technol. (2011).


CHAPTER
2

ISBN: 978-625-6971-51-6

A NEW APPROACH TO SUPERPOSITION OPERATORS ON SOME NON-NEWTONIAN MADDOX SEQUENCE SPACES

Dr. Fatmanur ERDOĞAN
Ondokuz Mayıs University, Samsun, Turkey
ORCID:0000-0001-5638-5294

Prof. Birsen SAĞIR, Ph.D
Ondokuz Mayıs University, Samsun, Turkey
ORCID:0000-0001-5954-2005

1. INTRODUCTION

The beginning of non-Newtonian calculus is based on Grossman and Katz [11]. They wrote the book that laid the foundations for non-Newtonian calculus. Their book contains some different types of calculus such as bigeometric, quadratic, biquadratic, harmonic calculus and is accepted as a fundamental work in this area. Accordingly the recent literature, it is observed that interest in this topic has increased due to applications and usefullness in wide area, see [4,9,10,17,18,24]. Duyar et al. [8] constructed some topological properties for non-Newtonian real axis. Also, Değirmen [7] studied non-Newtonian version of C^*- algebras generalizes known C^*-algebras. On the other hand, Değirmen and Sağır [6] presented some topological and geometric features of l_p in bicomplex setting with according to the non-Newtonian calculus by defining non-Newtonian bicomplex versions of some known topological features of sequence spaces.

There is a considerable literature on superposition operators. Dedagich and Zabreiko [5] provided necessary and sufficient conditions for the action of the superposition operator on the space ℓ_p. One of the contributions to the superposition operator and integrable solutions of some functional equations dates back to Banas [2]. Sama-ae [22] and Tainchai [23] examined boundedness of superposition operators on some sequence spaces. Sağır and Güngör [19,20] studied continuity and boundedness of such operators on some double sequence spaces, and also in [12], Güngör and Sağır obtained characterizations on double sequence

spaces of Maddox $L(p)$. In other studies, the authors in [13,15,16] investigated some properties of superposition operators such as continuity, uniform continuity, etc. on the various spaces.

In addition to the articles, given above for sequence spaces and superposition operators, we refer to the standard books of Appell and Zabreiko[1] and Choudhary and Nanda [3].

Let $S(N)$ be a space of non-Newtonian real number sequences, Y_α be a sequence space on $\mathbb{R}_\alpha$ and Z_β be a sequence space on $\mathbb{R}_\beta$. A non-Newtonian superposition operator ${}_NP_h$ is a mapping from Y_α into $S(N)$ defined by ${}_NP_h(x)=(h(m,x_m))_{m=1}^{\infty}$ when $h:\mathbb{R}\times\mathbb{R}_\alpha\to\mathbb{R}_\beta$ provides condition (NA_1) as follows.

(NA_1) $h(m,0)=0$ for all $m\in\mathbb{R}$.

If ${}_NP_h\in Z_\beta$ for all $x=(x_m)\in Y_\alpha$, then ${}_NP_h$ acts from Y_α into Z_β and it is written as ${}_NP_h:Y_\alpha\to Z_\beta$.

In some cases, the function h will be deemed to meet the following conditions.

(NA_2) $h(m,.)$ is $*-$continuous for all $m\in\mathbb{R}$.

(NA_2') $h(m,.)$ is $*-$bounded on all $\alpha-$bounded subset of $\mathbb{R}_\alpha$ for every $m\in\mathbb{R}$ [21].

Let $p=(p_k)$ be a bounded sequence of positive numbers and $M=\max\left\{1,\sup_k p_k\right\}$ for $k\in\mathbb{N}$. Non-Newtonian Maddox sequence spaces are defined as follows.

$$\ell_{\infty,\alpha}(p)=\left\{(x_k):{}^{\alpha}\sup_k |x_k|_\alpha^{(p_k)_\alpha}<+\infty\right\}$$

$$c_{0,\alpha}(p)=\left\{(x_k):{}^{\alpha}\lim_{k\to\infty}|x_k|_\alpha^{(p_k)_\alpha}=0\right\}$$

$$c_\alpha(p)=\left\{(x_k):{}^{\alpha}\lim_{k\to\infty}|x_k-a|_\alpha^{(p_k)_\alpha}=0,\ a\in\mathbb{R}_\alpha\right\}$$

ISBN: 978-625-6971-51-6

Let $\|.\|_X : X \to \square_\alpha$ be defined by $\|x\|_X = {}^{\alpha}\sup_k |x_k|_\alpha^{\left(\frac{p_k}{M}\right)_\alpha}$ when $X \in \left\{\ell_{\infty,\alpha}(p), c_{0,\alpha}(p), c_\alpha(p)\right\}$. Let $d_\alpha : X \times X \to \square_\alpha$ be defined as $d_\alpha(x,y) = \|x - y\|_X$. Then d_α is non-Newtonian metric on X. Hence the non-Newtonian Maddox sequence spaces are non-Newtonian metric spaces under the metric induced by the function $\|.\|_X$.

Let $T \subset \square_\alpha$ be non-Newtonian real vector space and $f : T \to \square_\beta$ be a function. Then f is named a *-paranorm and the pair (T, f) is a *-paranormed space, if the following conditions are provided for all $v, y \in T$ and $\lambda \in \square_\alpha$.

(i) $f(v) = 0$ if $v = 0$.

(ii) $f(0 - v) = f(v)$.

(iii) $f(v + y) \leq f(v) + f(y)$.

(iv) Let (λ_m) be a sequence of $\alpha-$scalars and (y_m) be an $\alpha-$sequence for all $m \in \square$. Then $f(\lambda_m \times y_m - \lambda \times y) \xrightarrow{\beta} 0$ while $\lambda_m \xrightarrow{\alpha} \lambda$ and $f(y_m - y) \xrightarrow{\beta} 0$ for $m \to \infty$.

In addition, if $v = 0$ where $f(v) = 0$, then f is named *-total paranorm and (T, f) is named *-total paranormed space. Every *-total paranorm space is a *-linear metric space [3,14].

Motivated essentially by [22] and [23] in classical calculus, in this paper, we introduce the characterizations of superposition operators from non-Newtonian Maddox sequence spaces $\ell_{\infty,\alpha}(p), c_\alpha(p)$ and $c_{0,\alpha}(p)$ to $\ell_{1,\beta}$ under some hypotheses related to continuity of the function f. Also, we give some significant examples providing these with respect to the special calculus such as bigeometric calculus. Therefore, our approach carry characterizations of superposition operators and some related concepts from the recent literature in classical calculus to $*$-calculus.

2. MAIN RESULTS

Theorem 2.1: The non-Newtonian Maddox sequence space $c_{0,\alpha}(p)$ is a *-linear metric space according to the following *-paranorm

$$f(x)=\sup_{k\in\mathbb{N}}\left|\iota\left(x_k\right)\right|_\beta^{\left(\frac{p_k}{M}\right)_\beta} \tag{1}$$

If $\inf p_k>0$, the non-Newtonian Maddox sequence spaces $c_\alpha(p)$ and $\ell_{\infty,\alpha}(p)$ are *-linear metric spaces according to the *-paranorm indicated by (1).

Proof: Let $x=(x_k)\in c_{0,\alpha}(p)$.

(i) If $x=0$, it is obtained that $\sup_{k\in\mathbb{N}}\left|\iota\left(x_k\right)\right|_\beta^{\left(\frac{p_k}{M}\right)_\beta}=0$. So $f(x)=0$

.

Conversely, let $f(x)=0$. According to definition of the function f , $\iota(x_k)=0$ and so $x=0$.

(ii) $f(0-x)=\sup_{k\in\mathbb{N}}\left|\iota\left(0-x_k\right)\right|_\beta^{\left(\frac{p_k}{M}\right)_\beta}=\sup_{k\in\mathbb{N}}\left|\iota\left(x_k\right)\right|_\beta^{\left(\frac{p_k}{M}\right)_\beta}=f(x).$

(iii) For every $c,u\in c_{0,\alpha}(p)$

$$\begin{aligned}f(c+u)&=\sup_{k\in\mathbb{N}}\left|\iota\left(c_k+u_k\right)\right|_\beta^{\left(\frac{p_k}{M}\right)_\beta}\\&\le\sup_{k\in\mathbb{N}}\left|\iota\left(c_k\right)\right|_\beta^{\left(\frac{p_k}{M}\right)_\beta}+\sup_{k\in\mathbb{N}}\left|\iota\left(u_k\right)\right|_\beta^{\left(\frac{p_k}{M}\right)_\beta}\\&=f(c)+f(u).\end{aligned}$$

(iv) Let $b_n\xrightarrow{\alpha}b$ and $f(y_n-y)\xrightarrow{\beta}0$ for $n\to\infty$ where (b_n) is a sequence of $\alpha-$scalars and $(y_n)\in c_{0,\alpha}(p)$ for all $n\in\mathbb{N}$. For $|b_n|_\alpha^{\left(\frac{p_n}{M}\right)_\alpha}\le L,$

ISBN: 978-625-6971-51-6

$$f(b_n \times y_n - b \times y) = {}^{\beta}\sup_{n \in \mathbb{N}} \left| \iota(b_n \times y_n - b \times y) \right|_{\beta}^{\left(\frac{p_n}{M}\right)_{\beta}}$$

$$= {}^{\beta}\sup_{n \in \mathbb{N}} \left| \iota(b_n \times y_n - b_n \times y + b_n \times y - b \times y) \right|_{\beta}^{\left(\frac{p_n}{M}\right)_{\beta}}$$

$$\leq {}^{\beta}\sup_{n \in \mathbb{N}} \left| \iota(b_n \times y_n - b_n \times y) \right|_{\beta}^{\left(\frac{p_n}{M}\right)_{\beta}} + {}^{\beta}\sup_{n \in \mathbb{N}} \left| \iota(b_n \times y - b \times y) \right|_{\beta}^{\left(\frac{p_n}{M}\right)_{\beta}}$$

$$\leq \iota(L) \times {}^{\beta}\sup_{n \in \mathbb{N}} \left| \iota(y_n - y) \right|_{\beta}^{\left(\frac{p_n}{M}\right)_{\beta}} + \left| \iota(y) \right|_{\beta}^{\left(\frac{p_n}{M}\right)_{\beta}} \times {}^{\beta}\sup_{n \in \mathbb{N}} \left| \iota(b_n - b) \right|_{\beta}^{\left(\frac{p_n}{M}\right)_{\beta}}.$$

Hence the non-Newtonian Maddox sequence space $c_{0,\alpha}(p)$ is a *-linear metric space according to the following *-paranorm indicated by (1).

Theorem 2.2: There is the following relation between non-Newtonian Maddox sequence spaces.

$$c_{0,\alpha}(p) \subset c_{\alpha}(p) \subset \ell_{\infty,\alpha}(p)$$

Proof: Let $u \in c_{0,\alpha}(p)$. We write ${}^{\alpha}\lim_{k \to \infty} \left| u_k - a \right|_{\alpha}^{(p_k)_{\alpha}} = 0$ for $a = 0$. Then $u \in c_{\alpha}(p)$. Thus $c_{0,\alpha}(p) \subset c_{\alpha}(p)$.

Since $\alpha-$convergent sequence is $\alpha-$bounded it is written that ${}^{\alpha}\sup_{k \in \mathbb{N}} \left| u_k \right|_{\alpha}^{(p_k)_{\alpha}} < +\infty$. Then $u = (u_k) \in \ell_{\infty,\alpha}(p)$. So, the theorem is proved.

Theorem 2.3: Let $f : \mathbb{C} \times \mathbb{C}_{\alpha} \to \mathbb{C}_{\beta}$ provide the (N, A_2). ${}_{N}P_f : \ell_{\infty,\alpha}(p) \to \ell_{1,\beta}$ iff there is a $\beta-$sequence $(\psi_k) \in \ell_{1,\beta}$ for each $\alpha-$number $\mu > 0$ such that

$$\left| f(k,t) \right|_{\beta} \leq \psi_k \text{ while } \left| t \right|_{\alpha}^{\left(\frac{p_k}{M}\right)_{\alpha}} \leq \mu$$

for each $k \in \mathbb{N}$.

Proof: Suppose that ${}_{N}P_f : \ell_{\infty,\alpha}(p) \to \ell_{1,\beta}$. Let $\mu > 0$. Let we define $K(\mu)$ and $R(k,\mu)$ as

$$K(\mu)=\left\{t\in\square_\alpha:|t|_\alpha^{\left(\frac{p_k}{M}\right)_\alpha}\le\mu\right\}$$

$$R(k,\mu)=\sup_\beta\left\{|f(k,t)|_\beta:t\in K(\mu)\right\}$$

for each $k\in\square$. Therefore it is written that $|f(k,t)|_\beta\le R(k,\mu)$ whenever $|t|_\alpha^{\left(\frac{p_k}{M}\right)_\alpha}\le\mu$. Assume that there exits an $\alpha-$number $\mu_0>0$ such that $\left(R(k,\mu_0)\right)_{k=1}^\infty\notin\ell_{1,\beta}$. Then $\sum_{k=1}^\infty R(k,\mu_0)=+\infty$. Then there is a sequence of positive integers $\eta_0=0<\eta_1<\eta_2<...<\eta_i<...$ such that $\sum_{k=\eta_{i-1}+1}^{\eta_i}R(k,\mu_0)>1$ for all $i\in\square$. Also there is a $\beta-$number $\varepsilon_i>0$ such that

$$\sum_{k=\eta_{i-1}+1}^{\eta_i}R(k,\mu_0)-(\eta_i-\eta_{i-1})\times\varepsilon_i>1. \qquad (2)$$

Let $i\in\square$ be fixed. Since the function f provides the condition $(N4_2)$, it is written that $0\le R(k,\mu_0)<+\infty$ when $\eta_{i-1}+1\le k\le\eta_i$. There is $x_k\in K(\mu_0)$ such that

$$|f(k,x_k)|_\beta>R(k,\mu_0)-\varepsilon_i \qquad (3)$$

by the definition of $R(k,\mu_0)$. From (2) and (3), we get

$$\sum_{k=\eta_{i-1}+1}^{\eta_i}|f(k,x_k)|_\beta>\sum_{k=\eta_{i-1}+1}^{\eta_i}R(k,\mu_0)-\sum_{k=\eta_{i-1}+1}^{\eta_i}\varepsilon_i>1$$

for each $i\in\square$. Thus it is obtained that $\left(f(k,x_k)\right)_{k=1}^\infty\notin\ell_{1,\beta}$. Since $|x_k|_\alpha^{\left(\frac{p_k}{M}\right)_\alpha}\le\mu_0$ for all $k\in\square$, it is obtained that $(x_k)\in\ell_{\infty,\alpha}(p)$. It be in contradiction with the assumption. Hence $\left(R(k,\mu)\right)_{k=1}^\infty\in\ell_{1,\beta}$. The proof is completed taking $R(k,\mu)=\psi_k$.

ISBN: 978-625-6971-51-6

Let $x=(x_k)\in\ell_{\infty,\alpha}(p)$. Then these exists an α–number $\gamma>0$ such that $|x_k|_\alpha^{\left(\frac{p_k}{M}\right)_\alpha}\leq\gamma$ for every $k\in\mathbb{N}$. According to the hypothesis, there is a β–sequence $(\psi_k)\in\ell_{1,\beta}$ such that $|f(k,x_k)|_\beta\leq\psi_k$ for each $k\in\mathbb{N}$. Then we get

$$\beta\sum_{k=1}^{\infty}|f(k,x_k)|_\beta\leq\beta\sum_{k=1}^{\infty}\psi_k=\beta\sum_{k=1}^{\infty}|\psi_k|_\beta=\|(\psi_k)\|_{\ell_{1,\beta}}.$$

Then ${}_NP_f(x)\in\ell_{1,\beta}$, since ${}_NP_f(x)=(f(k,x_k))_{k=1}^{\infty}$. So ${}_NP_f$ is a non-Newtonian superposition operator which acts from α–Maddox sequence space $\ell_{\infty,\alpha}(p)$ to β–sequence space $\ell_{1,\beta}$.

Example 2.4: Let $\phi:\mathbb{R}\times\mathbb{R}_\alpha\to\mathbb{R}_\beta$ be as follows $\phi(k,t)=\frac{|2\times t(t)-5|_\beta^{(p_k)_\beta}}{6^{k_\beta}}\beta$ for every $k\in\mathbb{N}$ and for every $t\in\mathbb{R}_\alpha$. Since for each $k\in\mathbb{N}$ $\phi(k,.)$ is *-continuous function, it is obtained that ϕ provides the property (NA_2). Since

$$|2\times t(t)-5|_\beta^{\left(\frac{p_k}{M}\right)_\beta}\leq\left(2\times|t(t)|_\beta\right)^{\left(\frac{p_k}{M}\right)_\beta}+5^{\left(\frac{p_k}{M}\right)_\beta}\leq\left(2\times|t(t)|_\beta\right)^{\left(\frac{p_k}{M}\right)_\beta}+5,$$

it is written that

$$|2\times t(t)-5|_\beta^{(p_k)_\beta}\leq\left(\left(2\times|t(t)|_\beta\right)^{\left(\frac{p_k}{M}\right)_\beta}+5\right)^{M_\beta}.$$

Let $\mu>0$ and $t\in\mathbb{R}_\alpha$ with $|t|_\alpha^{\left(\frac{p_k}{M}\right)_\alpha}\leq\mu$. So $|t(t)|_\beta^{\left(\frac{p_k}{M}\right)_\beta}\leq t(\mu)$. Then for each $k\in\mathbb{N}$,

$$|\phi(k,t)|_\beta = \frac{|2\times t(t)-5|_\beta^{(p_k)_\beta}}{6^{k_\beta}}\beta \le \frac{\left(\left(2\times|t(t)|_\beta\right)^{\left(\frac{p_k}{M}\right)_\beta}+5\right)^{M_\beta}}{6^{k_\beta}}\beta \le \frac{|2\times t(\mu)+5|_\beta^{(M)_\beta}}{6^{k_\beta}}\beta.$$

Since

$$\beta\sum_{k=1}^{\infty}\frac{\left(2\times t(\mu)+5\right)^{M_\beta}}{6^{k_\beta}}\beta = \left(2\times t(\mu)+5\right)^{M_\beta}\times\beta\sum_{k=1}^{\infty}\frac{1}{6^{k_\beta}}\beta = \frac{\left(2\times t(\mu)+5\right)^{M_\beta}}{5}\beta,$$

we get that $(c_k)\in\ell_{1,\beta}$ putting $c_k=\frac{\left(2\times t(\mu)+5\right)^{M_\beta}}{6^{k_\beta}}\beta$ for all $k\in\mathbb{N}$. Hence ${}_NP_\phi$ acts from α-Maddox sequence space $\ell_{\infty,\alpha}(p)$ to $\ell_{1,\beta}$ by Theorem 2.3.

Theorem 2.5: Let function $f:\mathbb{N}\times\mathbb{R}_\alpha\to\mathbb{R}_\beta$ satisfy the condition (NA_2'). The non-Newtonian superposition operator ${}_NP_f$ acts from α–Maddox sequence space $c_\alpha(p)$ to β–sequence space $\ell_{1,\beta}$ iff there are $\mu>0$ and $(a_m)\in\ell_{1,\beta}$ such that

$$|f(m,t)|_\beta \le a_m \text{ where } |t-v|_\alpha^{\left(\frac{p_m}{M}\right)_\alpha}\le\mu$$

for each $m\in\mathbb{N}$ and for each $v\in\mathbb{R}_\alpha$.

Proof: Let $x=(x_m)\in c_\alpha(p)$. Then $\lim_{m\to\infty}|x_m-a|_\alpha^{(p_m)_\alpha}=0$ for an $a\in\mathbb{R}_\alpha$. By the hypothesis, there are $\delta>0$ and $(a_m)\in\ell_{1,\beta}$ such that

ISBN: 978-625-6971-51-6

$$|f(m,t)|_\beta \le \omega_m \text{ where } |t-a_\alpha^{\left(\frac{p_m}{M}\right)_\alpha}| \le \delta \qquad (4)$$

for each $m \in \mathbb{N}$. Since $\lim_{m\to\infty}{}^{\alpha}|x_m - a_\alpha^{(p_m)_\alpha}| = 0$, there is a $r \in \mathbb{N}$ with $|x_m - a_\alpha^{(p_m)_\alpha}| \le \delta^{M_\alpha}$ for all $m \ge r$. Hence $|x_m - a_\alpha^{\left(\frac{p_m}{M}\right)_\alpha}| \le \delta$. From (4), it is found that

$$\beta\sum_{m=r}^{\infty}|f(m,x_m)|_\beta \le \beta\sum_{m=r}^{\infty}\omega_m \le \beta\sum_{m=1}^{\infty}|\omega_m|_\beta = \|(\omega_m)\|_{\ell_{1,\beta}}.$$

Then $\beta\sum_{m=1}^{\infty}|f(m,x_m)|_\beta < +\infty$. It is found that ${}_NP_f(x) \in \ell_{1,\beta}$ since ${}_NP_f(x) = (f(m,x_m))_{m=1}^{\infty}$. Therefore we get ${}_NP_f : c_\alpha(p) \to \ell_{1,\beta}$.

Conversely, let ${}_NP_f : c_\alpha(p) \to \ell_{1,\beta}$ and $v \in \mathbb{C}_\alpha$ for each $\mu > 0$ and for each $m \in \mathbb{N}$, we describe

$$K(v,\mu) = \left\{t \in \mathbb{C}_\alpha : |t - v|_\alpha^{\left(\frac{p_m}{M}\right)} \le \mu\right\}$$

$$L(m,\mu) = {}^{\beta}\sup\left\{|f(m,t)|_\beta : t \in K(v,\mu)\right\}.$$

Then it is written that $|f(m,t)|_\beta \le L(m,\mu)$ whenever $|t - v|_\alpha^{\left(\frac{p_m}{M}\right)} \le \mu$. It is enough to show that $\lim_{m\to\infty}{}^{\alpha}|x_m - v|_\alpha^{(p_m)_\alpha} = 0$ α–number $\xi > 0$ such that $(L(m,\xi))_{m=1}^{\infty} \in \ell_{1,\beta}$. On the contrary, we consider that $(L(m,\mu))_{m=1}^{\infty} \notin \ell_{1,\beta}$ for all $\mu > 0$. So, for every $n \in \mathbb{N}$, $\beta\sum_{m=1}^{\infty}\left|L\left(m,3^{-n}\right)\right|_\beta = +\infty$. Therefore a sequence of positive integers $k_0 = 0 < k_1 < k_2 < \ldots < k_n < \ldots$ such that $\beta\sum_{m=k_{n-1}+1}^{k_n}\left|L\left(m,3^{-n}\right)\right| > 1$ for every $n \in \mathbb{N}$. Also there is an $\varepsilon_n > 0$ such that

$$\beta\sum_{m=k_{n-1}+1}^{k_n} L\left(m,3^{(-\eta)_\alpha}\right)\le\left(k_n-k_{n-1}\right)\times\varepsilon_n<1. \qquad (5)$$

Let $n\in\mathbb{N}$ be fixed. It is obtained that $0\le L\left(m,3^{(-\eta)_\alpha}\right)<+\infty$ for all $m\in\mathbb{N}$ with $k_{n-1}+1\le m\le k_n$, since f satisfies the property (NA_2'). So there is a $x_m\in K\left(v,3^{(-\eta)_\alpha}\right)$ such that

$$|f(m,x_m)|_\beta>L\left(m,3^{(-\eta)_\alpha}\right)-\varepsilon_n. \qquad (6)$$

By (5) and (6),

$$\beta\sum_{m=k_{n-1}+1}^{k_n}|f(m,x_m)|_\beta>\beta\sum_{m=k_{n-1}+1}^{k_n}L\left(m,3^{(-\eta)_\alpha}\right)-\beta\sum_{m=k_{n-1}+1}^{k_n}\varepsilon_n>1$$

for $n\in\mathbb{N}$. Therefore it is obtained that $\left(f(m,x_m)\right)_{m=1}^{\infty}\notin\ell_{1,\beta}$. Since $x_m\in K\left(v,3^{(-\eta)_\alpha}\right)$ with $k_{n-1}+1\le m\le k_n$, we have $|x_m-v|_\alpha^{\left(\frac{p_m}{M}\right)_\alpha}\le 3^{(-\eta)_\alpha}$ and $|x_m-v|_\alpha^{(p_m)_\alpha}\le 3^{(-\eta M)_\alpha}\le 3^{(-\eta)_\alpha}$. Thus $\alpha\lim_{m\to\infty}x_m-v|_\alpha^{(p_m)_\alpha}=0$ and $(x_m)\in c_\alpha(p)$. This is a contradiction. So there is a $\xi>0$ such that $\left(L(m,\xi)\right)_{m=1}^{\infty}\in\ell_{1,\beta}$. Hence we complete the proof by putting $\omega_m=L(m,\xi)$ for all $m\in\mathbb{N}$.

Example 2.6: In bigeometric calculus, $\alpha=\exp$ and $\beta=\exp$, let $h:\mathbb{R}\times\mathbb{R}_\alpha\to\mathbb{R}_\beta$ satisfies $h(k,t)=\frac{|t|_\beta^{(3p_k)_\beta}}{5^{(k+1)_\beta}}\beta$ for every $k\in\mathbb{N}$ and for every $t\in\mathbb{R}_\alpha$. Then $h:\mathbb{N}\times\mathbb{R}^+\to\mathbb{R}^+$ and $h(k,t)=e^{\frac{|\ln t|^{3p_k}}{5^{(k+1)}}}$. Since $h(k,.)$ is bi-geometric continuous function for all $k\in\mathbb{N}$, h satisfies the property (NA_2'). Let take any $v>0$ and let $t\in\mathbb{R}^+$ with $|t-v|_\alpha^{\left(\frac{p_k}{M}\right)_\alpha}\le\mu$. Let $\mu=e$. Since

ISBN: 978-625-6971-51-6

$|t-v|_\alpha^{\left(\frac{p_k}{M}\right)_\alpha}=e^{\left|\ln\frac{t}{v}\right|^{\left(\frac{p_k}{M}\right)}}\le e,$ it is obtained that $|\ln t-\ln v|^{\frac{p_k}{M}}\le 1.$ Therefore we write $|\ln t|^{\frac{p_k}{M}}\le 1+|\ln v|$ and also $|\ln t|^{3p_k}\le\left(1+|\ln v|\right)^{3M}.$ For each $k\in\mathbb{N}$

$$|h(k,t)|_\beta=\exp\left|\ln e^{\frac{|\ln t|^{3p_k}}{5^{(k+1)}}}\right|\le e^{\frac{\left(1+|\ln v|\right)^{3M}}{5^{(k+1)}}}$$

and $\beta\sum_{k=1}^{\infty}e^{\frac{\left(1+|\ln v|\right)^{3M}}{5^{(k+1)}}}=e^{\frac{\left(1+|\ln v|\right)^{3M}}{20}}$. Hence choosing $(c_k)=e^{\frac{\left(1+|\ln v|\right)^{3M}}{5^{(k+1)}}}\in\ell_{1,\beta}$ for all $k\in\mathbb{N}$, we get that ${}_NP_h:c_\alpha(p)\to\ell_{1,\beta}$ by Theorem 2.5.

Since $c_{0,\alpha}(p)\subset c_\alpha(p)$, the following result is obtained by taking $v=0$ in Theorem 2.5.

Corollary 2.7: Let function $f:\mathbb{N}\times\mathbb{N}_\alpha\to\mathbb{N}_\beta$ satisfy the condition $(N\Lambda_2)$. Then ${}_NP_f:c_{0,\alpha}(p)\to\ell_{1,\beta}$ iff there are $\theta>0$ and $(u_k)\in\ell_{1,\beta}$ such that

$$|f(k,z)|_\beta\le u_k \text{ whenever } |z|_\alpha^{\left(\frac{p_k}{M}\right)_\alpha}\le\theta$$

for each $k\in\mathbb{N}$.

REFERENCES

[1]Appell, J. & Zabreiko, P.P. (1989). *Nonlinear Superposition Operators*, Cambridge University Press, Cambridge.

[2]Banaś, J. (1988). On the Superposition Operator and Integrable Solutions of Some Functional Equations. *Nonlinear Analysis*, 12(8), 777-784.

[3]Choudhary, B. & Nanda, S. (1987). *Functional Analysis with Applications*, John Wiely, Sons, New Delhi, India.

[4]Çakmak, A. F. & Başar F. (2012). Some New Results on Sequence Spaces with Respect to Non-Newtonian Calculus. *Journal of Inequalities and Applications*, 228,1-12.

[5]Dedagich, F. & Zabreiko, P.P. (1987). Operator Superpositions in the Spaces *lp*. *Sibirskii Matematicheskii Zhurnal*, 28, 86-98.

[6]Değirmen, N. & Sağır, B. (2022). Some fundamental properties of Banach spaces $l_p\left(\mathbb{BC}\left(N\right)\right)$ with the *-norm $\left\|.\right\|_{2l_p\left(\mathbb{BC}\left(N\right)\right)}$. *Transactions of A. Razmadze Mathematical Institute*, 176(2), 183-195.

[7]Değirmen, N. (2022). Non-Newtonian Approach to C^*-Algebras. *Communications in Algebra*, 50(6), 2653-2671.

[8]Duyar, C., Sağır, B. & Oğur, O. (2015). Some Basic Topological Properties on Non- Newtonian Real Line. *British Journal of Mathematics and Computer Science*, 9:4, 300-307.

[9]Duyar, C. & Erdoğan, M. (2016). On Non-Newtonian Real Number Series. *IOSR Journal of Mathematics*, 12:6, IV, 34-48, doi: 0.9790/5728-1206043448.

[10]Erdoğan, M. & Duyar, C. (2018). Non-Newtonian Improper Integrals. *Journal of Science and Arts*, 1(42), 49-74.

[11]Grossman, M. & Katz, R. (1972). *Non-Newtonian Calculus*, 1st ed., Lee Press, Pigeon Cove Massachussets.

[12]Güngör, N. & Sağır, B. (2017). Continuity of Superposition Operators on Double Sequence Spaces of Maddox $L\left(p\right)$. *Iranian Journal of Science and Technology Transactions A: Science*, doi:10.1007/s40995-017-0266-1.

[13]Herawati, E. & Mursaleen, M. (2020). Superposition Operators on Some New Type of Order Modular Spaces. *Annals of the University of Craiova - Mathematics and Computer Science Series*, 47(2), 285-293.

[14]Kadak, U., Kirişci M. & Çakmak A. F (2015). On the Classical Paranormed Sequence Spaces and Related Duals over the Non-Newtonian Complex Field. *Journal of Function Spaces*, doi: 10.1155/2015/416906.

ISBN: 978-625-6971-51-6

[15] Oğur, O. (2020). Superposition operators on sequence spaces $\ell_p(F)$ derived by using matrix of Fibonacci numbers. *Linear and Multilinear Algebra*, 68(10), 2087-2098.

[16] Petranuarat, S. & Kemprasit, Y. (1997). Superposition Operators of ℓ_p and c_0 into ℓ_q $(1\leq p,q<\infty)$. *Southeast Asian Bulletin of Mathematics*, 21, 139-147.

[17] Sager, N. & Sağır, B. (2021). Some inequalities in quasi-Banach algebra of non-Newtonian bicomplex numbers. *Filomat*, *35*(7), 2231-2243.

[18] Sager, N. & Sağır, B. (2021). Banach spaces $l_p(\mathbb{BC}(N))$ with the *-norm $\|.\|_{2,l_p(\mathbb{BC}(N))}$ and some properties. *Tbilisi Mathematical Journal*, *14*(2), 65-81.

[19] Sağır, B. & Güngör, N. (2015). Continuity of Superposition Operators on the Double Sequence Spaces L_p. *Filomat*, 9, 2017-2118.

[20] Sağır, B. & Güngör, N. (2015). Locally Boundedness and Continuity of Superposition Operators on the Double Sequence Spaces C_{r0}. *Journal of Computational Analysis and Applications*, 19(2), 365-377.

[21] Sağır, B. & Erdoğan, F. (2019). On Characterization of Non-Newtonian Superposition Operators in Some Sequence Spaces. *Filomat*, 33(9), 2601-2612.

[22] Sama-ae, A. (1997). Boundedness of Superposition Operators on the Sequence Spaces of Maddox, Master of Sciences Dissertation, Graduate School of Chiang Mai University, 55, Thailand.

[23] Tainchai, P. (1996). Boundedness of Superposition Operators on Some Sequence Spaces, Master of Sciences Dissertation, Graduate School of Chiang Mai University, 40, Thailand.

[24] Torres, D. F. M. (2021). On a Non-Newtonian Calculus of Variations. *Axioms*, 10(3), 171.


CHAPTER
3

ISBN: 978-625-6971-51-6

CYDONIA OBLONGA MILL.: THE EVALUATION OF THE LEAVES FOR BIOLOGICAL AND COLORING PROPERTIES AS A SUSTAINABLE FABRIC DYE

Prof. Tülin AŞKUN, Ph.D.
Department of Biology
Faculty of Sciences and Arts
University of Balikesir
ORCID:0000-0002-2700-1965

Ph.D. Student Pınar GÜNER
Department of Biology
Faculty of Sciences and Arts
University of Balikesir
ORCID:0000-0001-6922-7009

Prof. Gülendam TÜMEN, Ph.D.
Department of Biology
Faculty of Sciences and Arts
University of Balikesir
ORCID:0000-0002-7457-3341

Prof. Fatih SATIL Ph.D.
Department of Biology
Faculty of Sciences and Arts,
University of Balikesir
ORCID:0000-0002-4938-1161

1. INTRODUCTION

1.1 Natural dyes

Natural dyeing application started in all cultures 15,000 years ago and continued intensely until the middle of the 19th century when synthetic dyestuffs were discovered. After the second half of this century, the use of synthetic dyestuffs, which adversely affected natural dyestuffs, made natural dyeing forgettable and brought it to extinction. It is a fact that natural dyes are not made anywhere in our country, except for a few major regions. Recently, great support has been given to the development of handicrafts using natural dyestuffs (Eyüpoğlu et al.,1983). Natural dyes have historical, cultural, and economic importance and value in the coloring of textile products. Each country has unique local natural dye resources. They have developed over the centuries through migrations and cultural and commercial exchanges. On the other hand, we have to accept that Anatolian natural dyeing, which has a rich tradition, consists of the synthesis of the information brought from the homeland and the oldest traditions of the rules coming from the 2nd century to nowadays (Eyüpoğlu et al., 1983). As a result of the increase in industrial production and research, many negative environmental effects such as climate change, pollution in air and water resources have emerged. Negative effects on ecology, decreasing water resources and problems related to chemical wastes necessitated the development of new and different alternatives in textile. These differences in approach include research carried out in a wide framework ranging from solar energy use to organic fiber selection, from environmentally friendly production methods to recycled fiber, water, dye, fabric, and natural dyes. They are used in many fields such as natural dyes, coloring textile products, pharmacy, cosmetics, and food. However, in natural dyeing, the continuity of raw materials and the excess amount used, difficulties in standardization, high cost and limitations in the color palette are among the most important problems encountered (Kayabaşı, 2000). Nevertheless, they can be obtained from renewable resources, and advantages such as being compatible with nature and easily degradable, protection from UV rays, and the anti-bacterial properties that make natural dyes attractive. Although natural dyes were generally considered to be of vegetable and animal origin and mineral-based in the past, nowadays, natural dyes obtained from bacteria / fungi / lichens are increasing, especially in the light of new research and developments. Among the natural dyestuffs, it is the plants that have a large place. It is used to paint various parts of plants called dye plants such as flowers, fruits, roots, leaves and stems. (Harmancıoğlu, 1973; 1955; Aydın, 1995; Kayabaşı, 2000).

ISBN: 978-625-6971-51-6

Rubia tinctorium (root dye) plant, which has names such as dye chili, dye root, dye litter, dye ivy, dye grass, tongue bleeding, red dye, red root, sticky and egg dye, is a dyestuff known since ancient Egyptians. The red dye obtained from the roots has been used as a fabric dye for a long time under the name of "Turkish red" or "Edirne red". In 1700, Turkey alone supplied two-thirds of the world's root dye needs. This drug lost its importance in a short time with the discovery of the technique of making alizarin, which is the main dyestuff of root dye, synthetically on a wide scale (Baytop, 1974; Kayabaşı et al., 1998; Uğur, 1988). Textiles as natural dyes of microbial pigments, and their use in dyeing are of interest. The current status and possible developments of microbial pigments as a natural dye source were evaluated by Tuli et al., (2015). Microbial pigments isolated *Curvularia lunata*, *Trichoderma virens*, and *Alternaria alternata* (Sharma et al., 2012); *Serratia marcescens* (Ren et al., 2018), and Talaromyces spp. (Oyervides et al., 2017) used in textile dyeing and obtained favourable results. Natural dyeing, which has regained its vitality today, has attracted the attention of many researchers in the last 10 years, and new studies have focused on researching the techniques of using natural dyes in the textile industry.

1.2 Main Factors Affecting Natural Dyeing Results

Type of natural dye source, drying method, used part, extraction method and conditions (water/chemical solvent usage, neutral/acidic/basic medium (pH), temperature, time), dyeing conditions (neutral/acidic/basic medium (pH), temperature, time) will be obtained are the main factors affecting the results. Mordants are natural compounds or other complexing agents containing metal salts and metal ions that improve dye uptake, fixation, and determine the resulting color and fastness properties. Color yield and coordinates are mordant types and highly dependent on the mordanting method. By creating a different dyestuff complex from each purple, it provides completely different colors and fastness properties (İşmal and Yıldırım, 2019). Depending on the type, type and mordanting method (pre-, simultaneous, post-mordanting) of the mordant, a wide range of different colors, darknesses, and color fastness values can be obtained with a natural dye. Many of the traditional mordant substances are salts of heavy metals such as aluminium, iron, copper, tin, and chromium. Their harmful effects on the environment and human health are criticized. While toxic metal salts such as copper sulfate and potassium bichromate were widely used in the past, these mordant substances are avoided due to the importance of ecological issues and they are almost banned. Limited use of them is permitted. Potassium aluminum sulfate (alum), aluminum sulfate, aluminum compounds such as aluminum acetate, and ferrous

compounds such as ferrous sulfate are ecologically safer and preferred metal mordants.

1.3. Functional Properties Added to Textile Products with Natural Dyes

Consumer expectations on health, hygiene, and comfort odour beautifying/preventive, anti-microbial, moth/insect/insect repellent, and UV protective finishing processes have also gained importance. The chemicals used to give these functional properties to textile products are criticized for ecological reasons and their effects on the environment. When we look at the studies carried out in recent years, there are many studies that show that natural dyestuffs can be used not only for coloring purposes but also to provide some functional finishing properties to textile products. Anti-microbial (Singh et al., 2005), pest-repellent with natural dyes (Kato et al., 2004), anti-odour (Hwang et al., 2008; Lee et al., 2008) textile products were obtained. With natural dyestuffs obtained from cheap waste materials, textile products can be given more than one functional property. Banana peels for dyeing cotton use anti-bacterial and UV rays at the same time protective properties were obtained (Salah, 2012). By examining the dyeing propeties and anti-bacterial activities of mordanted cotton and polyamide fabrics with natural dyes, it has been determined that they have excellent anti-bacterial properties (Shahidi, 2016). It has been shown that orange peel can also be used as a natural dye that absorbs UV rays (Hou et al., 2013). It has been reported that cotton, silk, and wool fabrics dyed with pomegranate peel extract have excellent deodorizing (Lee et al., 2013), and fabrics dyed with acorn (Lee, et al., 2015) both deodorizing and excellent antibacterial activity.

4 *Cydonia oblonga* Mill.

C. oblonga belongs to the Cydonia genus of the Pomoideae subfamily of the Rosaceae family is a plant. It is deciduous in winter and sometimes a shrub depending on its habitat. It has the appearance of a small tree, reaching 7-8 m in height. Young shoots with buds and 5-10 cm long, heart-shaped leaves are hairy. Chemically, quince leaves have dye in consists of xanthophyll which is a Dioxy-(Alpha)-carotene. Also called xanthophylline lutein. This substance gives the yellow color to the leaves in autumn gives. Quince is humous, dry, loamy, and permeable, It grows well in warm and irrigated soils. Homeland of the quince Caucasus, Iran, Turkestan, South Arabia, Italy, and Greece. It also grows in Yugoslavia, Bulgaria, and Turkey. Anatolia for many years. It was brought before and spread all over the country Sakarya in Turkey, Bursa, various cultural races, especially in Bilecik, Kocaeli, Ankara, Antalya, Manisa (domestic varieties Glass, Iron, Bread, Karaali, Lemon, Sugar, Crisp, Solitaire, foreign varieties Champion,

Fuller, Orange) are grown. Studies have shown that the phenolic compound concentration value in quince leaves is higher than other parts of the plant, and 17.31% of the total chemical content consists of tannins (Oliveira et al., 2008). Quince leaves are used as a sedative, anti-oxidant (free radical scavenger) and anti-pyretic among the people, apart from being a cheap and natural source of nutrition. Quince leaf extracts are also used in the treatment of various skin diseases due to their bioactive principles (Krstic-Pavlovic et al., 1983; Oliveira et al., 2012; Sajid et al., 2015). There are many studies in the field of textile dyeing with natural dyes (Carvalho and Santos, 2015). Natural dyeing studies with parts such as leaves and roots of plants in garden and forest areas are limited. The main polyphenolic components of these parts include flavonoids and tannins, allowing them to be used as a natural dye source (Kuppusamy et al., 2015).

In this study, anti-mycobacterial, anti-bacterial and anti-fungal effects, dyeing performances and anti-bacterial effects of dyed fabrics of ethanol extracts of *C. oblonga* leaves, which are considered natural waste, were determined. It is also intended to provide a detailed list of phenolic compounds. The results of this study are new since there is no literature on the anti-mycobacterial activities of *C. oblonga* leaves.

2.MATERIALS&METHODS

2.1 Preparation of extract

C. oblonga was collected from Cagis village, field Cagis village, field edges, 39°31'16.02"N, 28° 0'35.11"E, (26 m), 17.05.2014. Identification of the plant was made by Prof. Dr. Gülendam Tümen, Fatih Satıl and Selami Selvi. The plant used in the study is kept in the herbarium of the Biology Department of Balıkesir University (Herbarium Number: SV765). *C. oblonga* leaves were cut into small pieces and weighed. After the leaves were kept in ethanol extract at 25°C for two weeks, it was extracted, respectively. The extract was filtered through filter paper and evaporated with a rotary evaporator, the extract was preserved at -20 °C.

2.2 Microorganisms and Preparation of Cultures

Eight strains of bacteria used were *Bacillus cereus* (BC, ATCC 10876), *Staphylococcus aureus* (SA, ATCC 538), *Salmonella typhimurium* (ST, ATCC 14028), *Pseudomonas aeruginosa* (PA, ATCC 27853), *Klebsiella pneumonia* (KP, ATCC 31488), *Proteus vulgaris* (PV, ATCC 6897), Methicillin-resistant *Staphylococcus aureus* (MRSA, ATCC 33592) and *Escherichia coli* (EC, ATCC 8739). Five fungal pathogens, *Candida albicans* (CA, ATCC10239), *Aspergillus flavus* Link (AF, TA41-17), *Aspergillus ochraceus* K. Wilh (AO, MUCL 39534), *Aspergillus*

niger van Tiegh (AN, TA47-3), *Fusarium proliferatum* (FP, Matsushima, Nirenberg, TA18-2) were used. We investigated the anti-mycobacterial activities of extracts against four tuberculosis strains (MT-H37Ra, MT-H37Rv, and two clinical isolates). Invitro anti-bacterial activity efficiency was established by using MHA (Mueller Hinton Agar) and MHB (Mueller Hinton Broth) and anti-fungal activity assays SDA (Sabouraud Dextrose Agar) and SDB (Sabouraud Dextrose Broth). Anti-mycobacterial assays were used M7H9B (Middlebrook 7H9 Broth, Becton & Dickinson) and M7H10A (Middlebrook 7H10 Agar, Becton & Dickinson).

2.3 Anti-microbial sensitivity assays

2.3.1 Minimum inhibitory concentration assay (MIC)

MIC determination for the anti-bacterial and anti-fungal test, the microdilution method was used according to the National Committee for Clinical Laboratory Standards, Sensitivity Testing fungi and bacteria (NCCLS 2006; NCCLS 2008). In this study, the negative control well contains no organisms, while the positive control well contains organisms. Final concentrations in the wells ranged from 0.04 mg/mL to 25 mg/mL. For the incubation of all microplates, 24-48 hours at 37°C for bacteria and 72 hours at 28°C for fungi were selected. Then, Tiazolyl Blue Tetrazolium Bromide (TBTB, 20 µL, Sigma) was added to the wells and incubated at 37°C for an additional 4 hours. The color change in the solution was investigated. After the indicator dye turned pink, indicating positive bacteria growth, TBTB solution was added to the other wells. In the anti-mycobacterial activity, the MGIT guideline Fluorometric susceptibility test procedure was used for each sample (BD, 2002; NCCLS, 2003). For the production of *M. tuberculosis* strains incubated at 37 °C, 7H9 Broth Base (4 ml), OADC supplement (0.5 mL), and the antibiotic mixture of PANTA (0.1 mL) were used. The Mycobacterial activity of *C. oblonga* ethanol extracts in the test using Microplate Presto Blue Assay (MPBA). 198 µl of M7H9B and 2 µl of extract were added to the first column of each row. 100 µl of the medium was added to the other wells. Then, 20 µl of inoculum, excluding the negative control, was added to the wells and each microplate was incubated at 37°C for 5 days. The final extract concentration was in the range of 0.04-25 mg/mL. After incubation, the results were evaluated with 20 µl of Presto blue (Invitrogen, Life Technologies) solution. In the evaluation, the blue color in the well means no growth, and the pink color means positive growth. The MIC was determined as the lowest concentration at which the color did not turn pink and gave a negative result.

ISBN: 978-625-6971-51-6

2.3.2 Minimum bactericidal concentration Assay (MBC) and minimum fungicidal concentration Assay (MFC)

To determine MBCs and MFCs, bacteria or fungal suspension (20 µl) from the MIC and higher concentration wells were added to wells containing (80 µl) of fresh medium (MHB or SDB medium). To determine the MBC for *M. tuberculosis*, 80 µl of newly modified M7H9B was added. Experiments were performed in 3 repetitions.

2.4 Dyeing and Mordanting of Fabrics

After cold extraction with ethanol, the ethanol extracts were fed to the spray dryer or evaporation. After that, the fabric was dyed with *C. oblonga* leaves. In the dyeing process, 30/ 1 Rib and single jersey % 100 Cotton fabrics were used. In dyeing process were include pre-mordanting, washing, dyeing, washing, and drying in standard room conditions. Mordanting was performed utilizing $FeSO_4$, with tartaric acid, $CuSO_4$, and $KAl\ (SO_4)2.12H_2O$ in an aqueous solution. The color efficiency of dyed fabrics was measured in Sun Tekstil A.S. R&D Department in Izmir, Turkey.

2.5 Anti-bacterial Activity of Textile Materials

2.5.1 Microorganism and test specimens

Two strains of bacteria used were Gram (+) SA (ATCC 538) and Gram (-) KP (ATCC 31488). The stock culture was maintained on a NA at 4 ºC in the refrigerators. Test specimens (non-sterile) were cut by hand as rectangular specimens approximately cut 25 × 50 mm.

2.5.2 Anti-bacterial test method

This method is applied quickly and easily to determine the anti-bacterial activity of anti-microbial agents that can spread on treated textile materials (AATCC Test Method, 2008). If a diffusible antimicrobial agent has anti-bacterial activity, a zone of inhibition is formed; accordingly, bacterial growth is not observed at the borders of the sample and on the surface of the medium, which is in direct contact with the agar surface. During the application, five strips of 6 cm length and 10 mm intervals were drawn on the surface of the dish using a loopful of diluted inoculum. Test specimens were placed along the five inoculation lines with gentle pressure to make contact with the agar surface. Petri dishes were incubated at 37 °C for 18-24 hours. It was examined whether there was a growth interruption and a clear inhibition zone along the inoculum lines in the incubation plates. The mean width of the line and the inhibition zone on both sides of the test sample was measured.

2.6 HPLC Conditions

C. oblonga leaves ethanol extract was analyzed by HPLC (Shimadzu, autosampler SIL–20AHT). Mobile phases were %3 and %97 water (solvent A) and Methanol (solvent B). The detector used was a DAD (PD-M20A) (max = 800 nm) and the range of the maximum absorbance was 190-800 nm. The column temperature was 40°C and the injection volume was 20 µL. Standards of phenolic compounds were prepared by adapting the method prepared by Caponio et al., (1999).

3. RESULTS

In this study, eight bacteria and five fungi were used the determine the anti-bacterial and anti-fungal activities of the sample. The results of C. oblonga ethanol extract were given below in Table-1.

Table 1. Anti-bacterial and anti-fungal activity of leaves of *C. oblonga*

Anti-bacterial and Anti-fungal Activities		
Microorganisms	**MIC** (mg/ml)	**MBC/MFC** (mg/ml)
S. aureus	6.3	6.3
K. pneumoniae	1.6	6.3
E. coli	12.5	>25
B. cereus	6.3	>25
S. typhimurium	25	>25
P. vulgaris	25	>25
P. aeruginosa	12.5	25
MRSA	25	25
C. albicans	25	25
A. flavus	12.5	25
A. niger	12.5	25
A. ochraceus	12.5	25
F. proliferatum	3.1	12.5

ISBN: 978-625-6971-51-6

We also demonstrated the anti-mycobacterial activities of the extract against MT-Ra, MT- Rv and two clinical isolates using the MPBA. The results of the sample were given in Table-2.

Table 2. Anti-mycobacterial activity of leaves of *C. oblonga* ethanol extract (mg/mL).

Anti-mycobacterial Activity of *C. oblonga* (mg/mL) and Standart Drugs (µg/mL)						
	C. oblonga		**Isoniazid**		**Rifampisin**	
Microorganisms	**MIC**	**MBC**	**MIC**	**MBC**	**MIC**	**MBC**
MT-Ra	12.5	>25	0.13	1.04	0.64	5.12
MT-Rv	12.5	25	0.52	1.04	0.32	2.56
ST-1	25	>25	0.52	1.04	0.64	0.64
ST-2	25	>25	0.52	4.16	5.12	10.24

CIELAB values are used for the determination of the color; L* is used for perceptual clarity and a*- b* (red, green, blue, and yellow) for the four unique colors of human vision (Figure 1). As a result of dyeing with *C. oblonga* leaves extract, a color scale obtained ranging from dark purple to salmon pink and CIE color coordinates were given in Figure 2. The washing and water fastness of the samples dyed under the optimised conditions was tested according to the standard methods (Table 3).

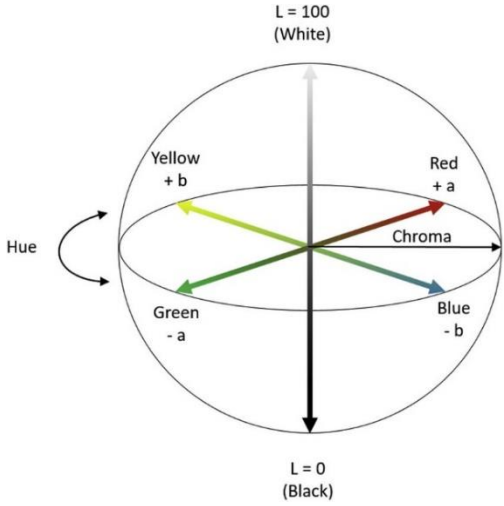


Figure 1. The CIELAB colour space diagram (Ly et. al.,2020).

Sample Name	Mordant	Leaves Amount (%)	Obtained Color	CIE color coordinates		
				L*	a*	b*
Q-1	**No-Mordant**	100		81,46	8,3	10,03
Q-2	**FeSO4 with tartaric acid**	100		66,43	7,15	6,57
Q-3	**$KAl(SO_4)_2.12H_2O$**	100		52.4	34.5	17.5
Q-4	**$CuSO_4$**	100		46,7	2,14	2,69

Figure 2. Fabric samples leaves of *C. oblonga* with or without mordants.

ISBN: 978-625-6971-51-6

Table 3. Fastnesses to water and washing of the colours obtained from leaves of *C. oblonga*

Fastness / NoMordant		KAl $(SO4)_2.12H_2O$	$CuSO_4$	$FeSO_4$ with tartaric acid
Washing Fastness	4/5	4/5	4/5	4/5
Water Fastness	4/5	4/5	4	4/5

The anti-microbial efficacy of the treated and untreated fabrics sample was determined by the parallel streak method (Figure 3).

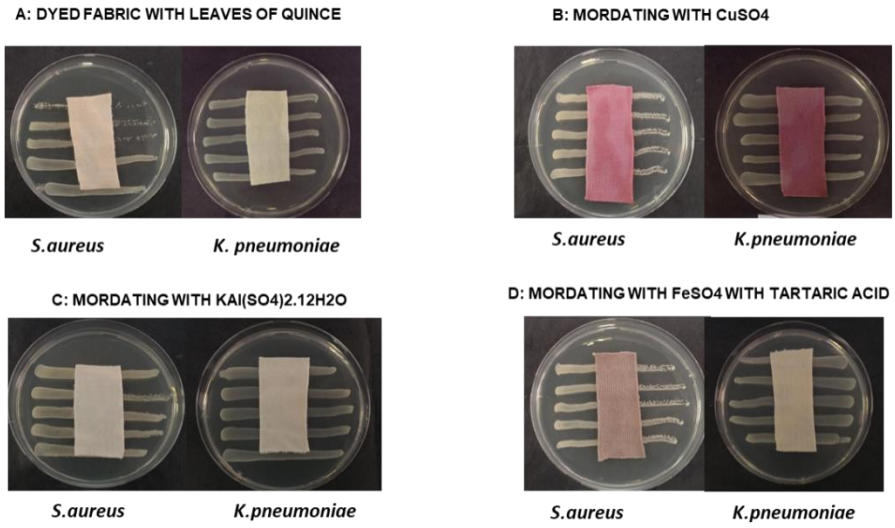


Figure 3. Assessment of anti-bacterial activity of *C. oblonga* on the fabrics.

The results of HPLC analyses of sample taken from *C. oblonga* was given in Table 4. The HPLC chromatogram of "*C. oblonga*" (Figure 4) was given below.

Table 4. Chemical composition of leaves of *C. oblonga s* ethanol extract (µg/mL).

no	Compound	Ret. Time	*C. oblonga*
1	Gallic Acid **(G-A)**	9.00	*
2	Chlorogenic Acid **(C-A)**	27.52	0,605
3	4-hydroxybenzaldehide **(4-HB)**	29.36	0,513
4	Vanilic Acid **(V-A)**	33.00	1,603
5	Cafeic Acid **(C-A)**	33.66	*
6	Epicatechin **(EC)**	34.44	*
7	Syringic Acid **(S-A)**	37.26	102,82
8	Echinocoside **(E)**	41.89	*
9	P-Coumaric Acid **(P-CA)**	40.70	0,43
10	Ferrulic Acid **(F-A)**	43.16.	0,48
11	Benzoic Acid **(B-A)**	48.14	*
12	2-Hydroxycinnamic Acid **(2-HA)**	48.73	0,48
13	Hesperidine **(H)**	49.55	*
14	Rutin Hydrate **(RH)**	50.42	*
15	Resveratrol **(R)**	52.24	0,76
16	Rosmarinic Acid **(R-A)**	52.89	12,94
17	Transcinnamic Acid **(T-A)**	59.12	0,31
18	Quercetine **(Q)**	61.74	*
19	Neochlorogenic Acid (**NC-A**)	18.26	22,95
20	Kuromanin Chloride **(KC)**	25.39	14,70
21	4-O-Caffeolquinic Acid **(4-O-C)**	28.67	20,70
22	Taxifolin **(T)**	42.63	6,86
23	Chicoric Acid **(CH-A)**	48.61	30,78
24	Ellagic Acid **(EL-A)**	50.99	*
25	Oleuropein **(O)**	51.93	*
26	Myricetin **(M)**	53.55	6,05
27	Luteolin **(L)**	64.25	7,42
28	Ursolic Acid **(U)**	46.41	*
29	Naringenin **(N)**	62.92	0,74
30	Apigenin-7-Glukozit **(A7G)**	52.45	*
31	Juglon **(J)**	57.86	*
32	Naringin **(Na)**	48.10	49,53
33	Kaempferol **(K)**	68.25	*

*Not peak detected

ISBN: 978-625-6971-51-6

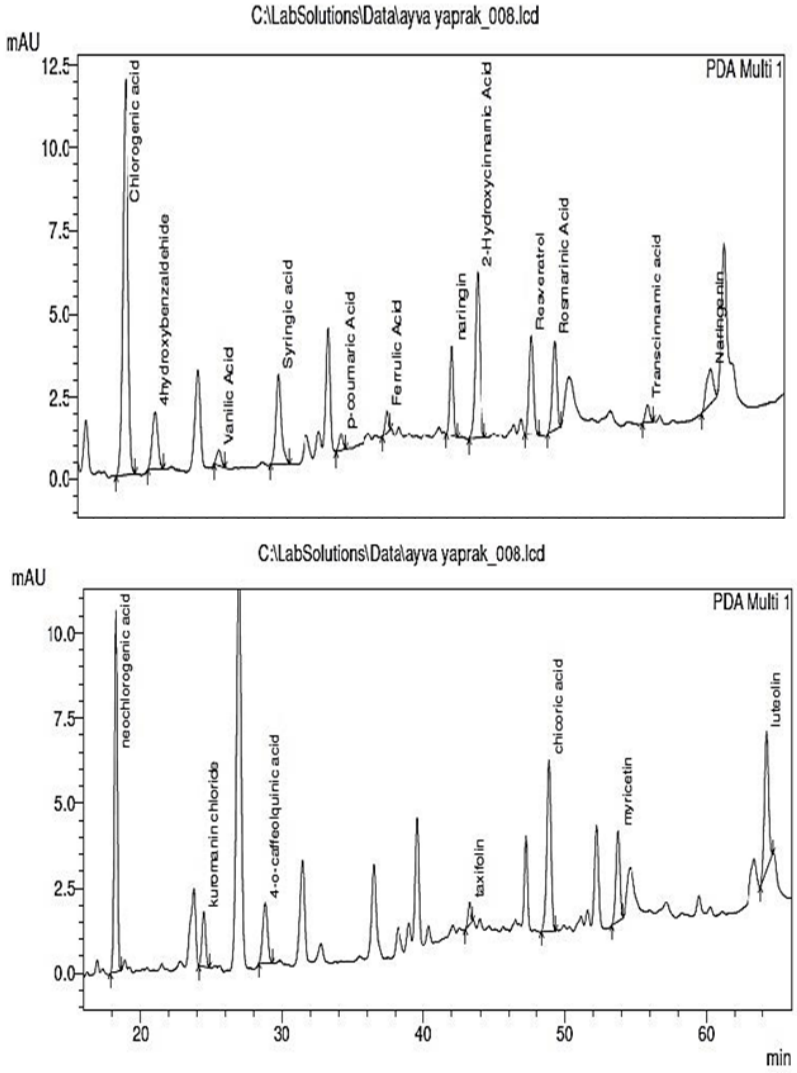


Figure 4. HPLC Chromatogram of leaves of *C. oblonga* ethanol extract.

∗ Retention time of the standards (min): C-A (27.52), 4-HB (29.36), V-A (33.00), S-A (37.26), P-CA (40.70), F-A (43.16), Na (48.10), 2-HA (48.73), R (52.24), R-A (52.89), T-A (59.12), N (62.92), NC-A (18.26), KC (25.39), 4-O-C (28.67), T (42.63), CH-A (48.61), M (53.55), L (64.25).

4.DISCUSSION

The *C. oblonga* leaves ethanol extract were successfully extracted by using a rotary evaporator. Sample stock solution and working solution were prepared by serial dilution with a concentration range of 0.04-25 mg/mL. While the lowest MIC values determined for quince extract were found against *K. pneumoniae* (MIC value was 3.1 mg/mL), the MBC was 6.3 mg/mL, respectively. The *C. oblonga* leaves ethanol extract exhibited the most significant activity against FP with a MIC value of 3.1 mg/ml, respectively. It is also determined that the quince extract was found to be efficacy against AF, AN and AO (MICs 12.5, MBCs 25 mg/mL). Various parts of plants (root, fruit, leaf and seed) are used in the treatment of some diseases (Budriesi et al., 2010) and these parts carry secondary metabolites (Rahmatullah et al., 2010 a, b;) (tannin, terpenoid, alkaloid) with therapeutic potential (Ghanbari et al., 2012). Quince leaves have many biological properties. Among these, hypercholesterolemia, protective effect on spermatogenesis (Ashrafi et al., 2013), protection against fungus (Hamid et al., 2013), antiatherogenic, and hepatoprotective effect (Khademi et al., 2013), preventive effect (Carvalho et al., 2010), renoprotective effect (Jouyban et al., 2011), and antioxidant potential (Costa et al., 2009) is essential. Various extracts (ethanol, acetone and aqueous) obtained from fruit and seeds were tested on four bacteria (*E. coli*, *K. pneumonia*, *S. aureus* and *Enterobacter aerogenes*). It was observed that the results for ethanol in the extracts were the best, the results for the aqueous extracts were less effective on bacteria (Alizadeh et al., 2013a). In addition, in results for quince seeds, the methanolic extract was found to be effective on various bacteria (*S. aureus*, *S. epidermidis* and *K. pneumonia*) (Al-khazraji, 2013). The antibacterial activities result of seeds and fruits are shown in another study by Alizadeh et al. (2013a) are similar to the results of the ethanol extract of the leaf in our study. In addition, quince leaf extracts (ethanol and acetone) showed antifungal effects on *A. niger* (Alizadeh et al., 2013b). However, in our study, the anti-fungal activity of *C. oblonga* was investigated and apart from *A. niger*, *F. proliferatum A. flavus*, and *A. ochraceus*. We obtained in our study are consistent with the antifungal activity results of Alizadeh et al., (2013b).

This study is the first report describing the anti-mycobacterial activity of *C. oblonga* leaves against patient strains, MT-Ra and MT-Rv. While the lowest MIC values determined for *C. oblonga* were found against MT-Ra, and MT-Rv (MICs value were 12.5 mg/mL), ST-1 and ST-2 showed the minimum MIC values. They have the same MIC and MBC values.

ISBN: 978-625-6971-51-6

In the ethanol extract of the sample, the major flavonoid was found to be S-A. Other major flavonoids were, R-A, NC-A, 4-O-C, CH-A and Na. As minor flavonoids, C-A, 4-HB, P-CA, F-A, and 2-HA were obtained in *C. oblonga* leaves respectively (Abbreviations in Table 4). It is thought that the presence of C-A in acetone and aqueous extracts (peel and pulp) of quince together with other components causes antimicrobial activity (Fattouch et al., 2007). The presence of C-A and anti-microbial activity results in our study support this study.

While the most abundant compound in the pulp of Tunisian quince (*Cydonia oblonga* Miller) was determined as chlorogenic acid (5-O-caffeoylquinic acid), the main component in the peel was determined as rutin (quercetin 3-O-rutinoside) (Fattouch et al., 2007).

Oliveria et al., (2007) investigated the leaves of Portuguese quince. The essential phenolics were 5-O-caffeoylquinic acid, 3,5-O-dicaffeoylquinic acid, 3-O-caffeoylquinic acid, 4-O-caffeoylquinic acid, quercitin-3-O-rutinoside, kaempferol-3-O-rutinoside, quercitin-3-O-galactoside, kaempferol-3-O-glycoside, and kaempferol-3-O-glucoside.

When our HPLC results were examined, it was seen that our data were similar to the data of Tunisian and Portuguese quince.

In this study, fabric dyeing was done with quince leaves and the anti-bacterial activities of the fabrics were tested. In this study, we used two factors for measuring the inhibition zone method: the anti-microbial activity of the samples against the microorganism and the capability of the antimicrobial agent to diffuse into the agar. The dyed fabric with quince leaves did not show anti-bacterial activity against SA and KP. However, ıt was observed that the extract diffused into the agar in the fabric samples dyed with *C. oblonga* leaf extract.

5. CONCLUSION

Today, research and perspectives on natural dye applications have gone far beyond traditional approaches. As a result of many interdisciplinary interactions such as physics, chemistry, biology, biotechnology, engineering, design, and art, natural dyes have gone beyond traditional applications and have been used in different fields for purposes that were not on the agenda before uses emerged. However, it is necessary to carry out technical analyzes such as the optimum use of many natural dye sources with different structural properties, laboratory studies, niche markets, and small-scale production, as well as increasing systematic research on adapting the data obtained from R&D studies to commercial and industrial production. As a result of all these studies, it can be thought that natural dyestuff may gain more industrial meaning and importance.

6. ACKNOWLEDGEMENTS

This study was financially supported by Ministry of Science, Industry and Technology SAN-TEZ R&D support program (SANTEZ project no: 0799.STZ.2011-1). We would like to thank Prof. Dr. Selami SELVİ for his help.

7. REFERENCES

AATCC Test Method 147-2004. (2008). Antibacterial activity assessment of textile materials: Parallel streak method. AATCC Technical Manual, American Association of Textile Chemists and Colorists, Research Triangle Park, NC.

Alizadeh, H., Rahnema, M., Semnanai, S. N., and Hajizadeh, N. (2013a). Detection of compounds and antibacterial effect of Quince (Cydonia oblonga Miller) extracts in vitro and in vivo. *J. Biol. Active Prod. Nat*., 3, 303–309. doi: 10.1080/22311866.2013.817731

Alizadeh, H., Ajalli, M., and Hossein, H. (2013b). Antifungal effect of Cydonia oblonga extracts on Aspergillus niger. *Jundishapur J. Microbiol.*, 2013, p4.

Al-khazraji, S. K. (2013). Phytochemical screening and antibacterial activity of the crude extract of Cydonia oblonga seeds. *Glob. Adv. Res. J. Microbiol*., 2, 137–140.

Ashrafi, H., Ghabili, K., Alihemmati, A., Jouyban, A., Shoja, M. M., Aslanabadi, S., et al. (2013). The effect of quince leaf (Cydonia oblonga Miller) decoction on testes in hypercholesterolemic rabbits: a pilot study. *Afr. J. Tradit. Complement. Alter. Med*., 10, 277–282. doi: 10.4314/ajtcam.v10i2.12

Aydın, H.S. (1995). *Soğan (Allium cepa L.) Bitkisinden Elde Edilen Renkler ve Bu Renklerin Yün Halı İplikleri Üzerindeki Isık ve Sürtünme Haslıkları*. (Yayınlanmamış yüksek lisans tezi). Ankara Üniversitesi /Fen Bilimleri Enstitüsü, Ankara.

Baytop, T. (1974). Farmokognazi, Cilt 2. İstanbul Üniversitesi Eczacılık Fakültesi: İstanbul.

Becton Dickinson and Company Newsletter BD. (2002). Bactec MGIT 960 SIRE kit now FDA-cleared for susceptibility testing of Mycobacterium tuberculosis. Microbiology News & Ideas, 13, 4-4

Budriesi, R., Ioan, P., Micucci, M., Micucci, E., Limongelli, V., and Chiarini, A. (2010). Stop Fitan: antispasmodic effect of natural extract of chestnut wood in guinea pig ileum and proximal colon smooth muscle. *J. Med. Food*, 13, 1104–1110. doi: 10.1089/jmf.2009.0210.

Caponio, F., Alloggio, V., Gomes, T. (1999). Phenolic compounds of virgin olive oil: influence of paste preparation techniques, *Food Chemistry*, 64 (2): 203-209. doi:10.1016/S0308-8146(98)00146-0.

Carvalho, M., Silva, B. M., Silva, R., Valentao, P., Andrade, P. B., and Bastos, M. L. (2010). First report on Cydonia oblonga Miller anticancer potential: differential antiproliferative effect against human kidney and

colon cancer cells. *J. Agric. Food Chem*., 58, 3366–3370. doi: 10.1021/jf903836k

Carvalhoa, C., Santos, G. (2015). Global communities, biotechnology and sustainable design – Natural/Bio dyes in textiles. *Procedia Manuf*., 3, 6557–6564.

Costa, R. M., Magalhaes, A. S., Pereira, J. A., Andrade, P. B., Valentao, P., Carvalho, M., et al. (2009). Evaluation of free radical-scavenging and antihemolytic activities of quince (Cydonia oblonga) leaf: a comparative study with green tea (Camellia sinensis). *Food Chem. Toxicol*., 47, 860–865. doi: 10.1016/j.fct.2009.01.019

Eyüboğlu, Ü., Okaygün, D., Yaras, F. (1983). *Doğal Boyalarla Yün Boyama Uygulamalı ve Geleneksel Yöntemler*. Özkur Basımevi: İstanbul.

Fattouch, S., Caboni, P., Coroneo, V., Tuberoso, C., Angioni, A., Dessi, S., Marzouki, N., Cabras, P. (2007). Antimicrobial activity of Tunisian quince (Cydonia oblonga Miller) pulp and peel polyphenolic extracts. *Journal agricultural Food Chemistry*, 55: 963-969.

Ghanbari, R., Anwar, F., Alkharfy, K. M., Gilani, A. H., and Saari, N. (2012). Valuable nutrients and functional bioactives in different parts of olive (Olea europaea L) a review. *Int. J. Mol. Sci*., 13, 3291–3340. doi: 10.3390/ijms13033291.

Hamid, H. F., Moezzi, A., Khouzani, M. A., MahmoudJanlou, Y., Niknejad, F., and Faramarzi, M. A. (2013). Synthetic dye decolorization by three sources of fungal laccase. Res. *J. Chem. Environ*., 17, 76–81.

Harmancıoğlu, M. (1955). *Türkiye'de Bulunan Önemli Bitki Boyalarından Elde Olunan Renklerin Çesitli Müessirlere Karsı Yün Üzerindeki Haslık Dereceleri*. Ankara Üniversitesi Ziraat Fakültesi Yayınları (s.77). Ankara Üniversitesi Basımevi: Ankara.

Harmancıoğlu, M. (1973). Lif Teknolojisi, Cilt 1. E.Ü. Ziraat Fakültesi: İzmir.

Hou, X., Chen, X., Cheng, Y., Xu, H., Chen, L., and Yang, Y. (2013). Dyeing and UV-Protection Properties of Water Extracts from Orange Peel, *Journal of Cleaner Production*, 52, 410- 419.

Hwang E.K., Lee Y.H., and Kim H.D. (2008). Dyeing, fastness, and deodorizing properties of cotton, silk, and wool fabrics dyed with gardenia, coffee sludge, Cassia tora. L., and pomegranate extracts, *Fibers and Polymers*, 9(3), 334-340.

İsmal, Ö.E., Yıldırım L. (2019). Metal mordants and biomordants. In Shahid ul-Islam - Bhupendra Singh Butola (Ed.), *The Impact and Prospects of Green Chemistryfor Textile Technology* (p.57-82), England: Elsevier, Woodhead Publishing.

Jouyban, A., Shoja, M. M., Ardalan, M. R., Khoubnasabjafari, M., Sadighi, A., Tubbs, R. S., et al. (2011). The effect of quince leaf decoction on renal injury induced by hypercholesterolemia in rabbits: a pilot study. *J. Med. Plants Res*., 5, 5291–5295.

Kato, H., Hata, T., Tsukada, and M. (2004). Potentialities of natural dyestuffs as antifeedants against varied carpet beetle, Anthrenus verbasci, *Japan Agricultural Research Quarterly*, 38, 241-251.

Kayabası, N., Arlı, M., Erdoğan, Z. (1998). Kökboya (Rubia tinctorium L.)'dan Elde Edilen Renkler ve Bu Renklerin Yün Halı İplikleri Üzerindeki Isık ve Sürtünme Haslıkları. *Ankara Üniversitesi Ziraat Fakültesi Tarım Bilimleri Dergisi*. 4(3), 84-90.

Kayabası, N., Sanlı, H.S. (2000). Soğan Kabuklarının Bitkisel Boyacılıkta Kullanımı. *Türk-Koop. Ekin Dergisi*, 4(14), 99-103.

Khademi, F., Danesh, B., Nejad, M. D., and Rad, J. S. (2013). The comparative effects of atorvastatin and quince leaf extract on atherosclerosis. Iran. *Red Cres. Med. J*., 15, 639–643. doi: 10.5812/ircmj.4030

Krstic-Pavlovic, N., Lukic, P., Jokanovic, M., Gorunovic, M. (1983). Contribution to the study of [chemical] components in the quince leaves (Cydonia oblonga Mill.). *Jugoslovensko Vocarstvo*, 17, 27–35.

Kuppusamy, S., Thavamani, P., Megharaj, M., Naidua, R. (2015). Bioremediation potential of natural polyphenol rich green wastes: a review of current research and recommendations for future directions. *Environ. Technol. Innov.*, 4, 17–28.

Lee, Y.H., Hwang E.K., Baek Y.M., and Kim H.D. (2015). Deodorizing function and antibacterial activity of fabrics dyed with gallnut (Galla Chinensis) extract. *Textile Research Journal*, 85(10), 1045-1054.

Lee, Y.H., Hwang E.K., Baek Y.M., Lee M.S., Lee D.J., Jung Y.J., and Kim H.D. (2013). Deodorizing and antibacterial performance of cotton, silk and wool fabrics dyed with Punica granatum L. Extracts. *Fibers and Polymers*, 14(9), 1445-1453.

Lee, Y.H., Hwang, E.K., Jung, Y.J., Do, S.K., and Kim, H.D. (2008). Dyeing and deodorizing properties of cotton, silk, wool fabrics dyed with Amur Corktree, Dryopteris crassirhizoma, Chrysanthemum boreale, *Artemisia extract., Journal of Applied Polymer Science*, 115, 2246-2253.

Ly, B., Chau, K., Dyer Ethan, B., Jessica, L., Feig, A. L., Chien, and Del Bino, S. (2020). Research Techniques Made Simple: Cutaneous Colorimetry: A Reliable Technique for Objective Skin Color Measurement. *Journal of Investigative Dermatology*, 140, 3e12; doi:10.1016/j.jid.2019.11.003.

National Committee for Clinical Laboratory Standards (NCCLS). (2006). National Committee for Clinical Laboratory Standards. Methods for Dilution Antimicrobial Susceptibility Tests for Bacteria That Grow Edition Aerobically; Approved Standard. Seventh Edition NCCLS Document M7-A7., Wayne, Pennsylvania, 26(2) 1-16.

National Committee for Clinical Laboratory Standards (NCCLS). (2003). Susceptibility Testing of Mycobacteria, Nocardiae, and Other Aerobic Actinomycetes; Approved Standard. NCCLS document M24-A [ISBN 1-56238-500-3]. NCCLS, 940 West Valley Road, Suite 1400, Wayne, Pennsylvania 19087-1898 USA.

Oliveira, A. P., Pereira, J. A., Andrade, P. B., Valentao, P., Seabra, R. M., and Silva, B. M. (2007). Phenolic profile of Cydonia oblonga Miller leaves, *J. Agric. Food Chem.*, 55, 7926–7930. doi: 10.1021/jf0711237

Oliveira, A.P., Costa, R.M., Magalhães, A.S., Pereira, J.A., Carvalho, M., Valentão, P., Andrade, P.B., Silva, B.M. (2012). Targeted metabolites and biological activities of Cydonia oblonga Miller leaves. *Food Res. Int*., 46, 496–504.

Oliveira, A.P., Pereira, J.A., Andrade, P.B., Valentão, P., Seabra, R.M., Silva, B.M. (2008). Organic acids composition of Cydonia oblonga Miller leaf. *Food Chem.*, 111, 393–399.

Oyervides, L.M., Oliveira, J., Gallagher, M. S., Zavala, A. M., and Montanez, J. C. (2017). Assessment of the dyeing properties of the pigments produced by Talaromyces spp., *Journal of Fungi*, 3(3), 38, 1-9.

Performance Standards for Antimicrobial Susceptibility Testing; Ninth Informational Supplement. NCCLS document M100-S9. (2008). Wayne, PA, National Committee for Clinical Laboratory Standards.

Rahmatullah, M., Ferdausi, D., Mollik, M. A. H., Jahan, R., Chowdhury, M. H., and Haque, W. M. (2010a). A survey of medicinal plants used by Kaverajes of Chalna area, Khulna District, Bangladesh. *Afr. J. Trad. Complement Alt. Med*, 7, 91–97.

Rahmatullah, M., Kabir, A. A. B. T., Rahman, M., Hossan, S., Khatun, Z., Khatun, A., et al. (2010b). Ethnomedicinal practices among a minority group of christians residing in Mirzapur village of Dinajpur District. *Bangladesh. Adv. Nat. Appl. Sci.*, 4, 45–51.

Ren, R., Gong, J., Fu, R., Zhang J., Fang, K., and Liu X. (2018). Antibacterial dyeing of silk with prodigiosins suspention produced by liquid fermentation, *Journal of Cleaner Production*, 201, 648-656.

Sajid, S.M., Zubair, M., Waqas, M., Nawaz, M., Ahmad, Z. (2015). A review on quince (Cydonia oblonga): a useful medicinal plant. *Global Veterinaria*, 14, 517–524.

ISBN: 978-625-6971-51-6

Salah, S. M. (2012). Antibacterial Activity and UV Protection Property of Some Egyptian Cotton Fabrics Treated with Aqueous Extract from Banana Peel. *International Journal of Clothing Science*, 1 (1),1-6.

Shahidi, S. (2016). Antibacterial Efficiency of Mordant-Treated Cotton and Polyamide Fabrics, Before and After Dyeing. *Journal of Natural Fibers*, 3(5), 507-519.

Sharma, D., Gupta, C., Aggarwa S., and Nagpal, N. (2012). Pigment extraction from fungus for textile dyeing, *Indian Journal of Fibre and Textile Research*, 37(1), 68-73.

Singh, R., Jain, A., Panwar, S., Gupta, D., and Khare, S.K. (2005). Antimicrobial activity of some natural dyes, *Dyes and Pigments*, 66, 99-102.

Tuli, H.S., Chaudhary, P., Beniwal, V., and Sharma, A.K. (2015). Microbial pigments as natural color sources: current trends and future perspectives, *Journal of Food Science and Technology*, 52, 4669-4678.

Uğur, G. (1988). *Türk Halılarında Doğal Renkler ve Boyalar*. Türkiye İs Bankası Kültür Yayınları Genel Yayın : Ankara.


CHAPTER
4

ISBN: 978-625-6971-51-6

GLUTATHIONE (GSH-GSSG)

Assistant Professor Ebru COTELI
Ahi Evran University
Vocational School of Health Services
ORCID: 0000-0002-9473-0914

1. GLUTATHIONE (GSH) STRUCTURE

Glutathione (γ-glutamylcysteine glycine), the low-molecular-weight molecule in organisms containing a thiol group, is a major tripeptide [1, 2]. The 3 amino acids that make up its structure are, respectively, glutamic acid, cysteine, and glycine [3].

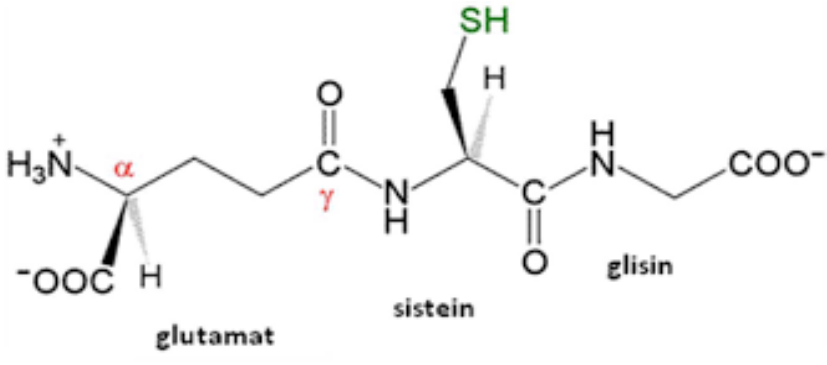


Figure 1. Structure of Glutathione (GSH)

In 1921, HOPKINS discovered glutathione, a sulfurous compound found in nature [4]. Glutathione exists in two forms, namely reduced glutathione (GSH) and oxidized glutathione (GSSG), which are in balance with each other in tissues [5].

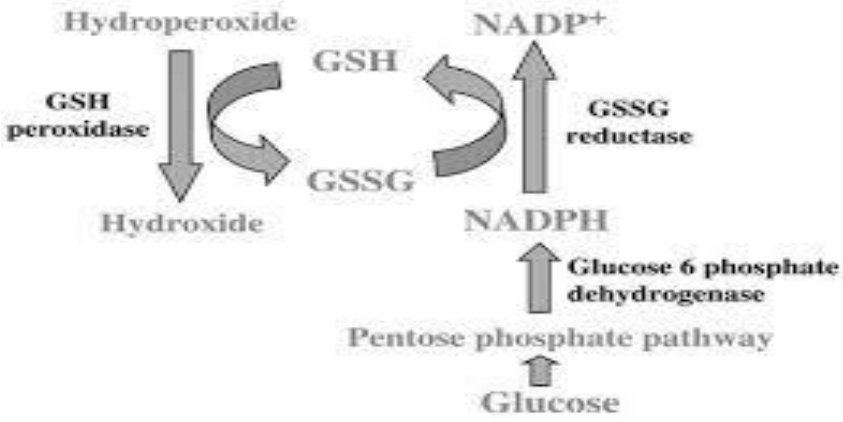


Figure 2. The cycle of glutathione (GSH-GSSG)

Glutathione, nearly all of which is synthesized in eukaryotic cells [6]. As a result, there are high densities. Approximately 85–90% of glutathione is in the cytoplasm, which is also available. But sometimes GSH is in the cytoplasm. After synthesis, the nucleus, peroxisomes, and endoplasmic reticulum can also be found [7, 8].

Glutathione is involved in the structure of the glyoxalase coenzyme. This coenzyme is involved in oxygen transport in tissues [9]. Glutathione has a structure that can easily give and take hydrogen. With this feature, it contributes to various redox events. Moreover, it inhibits the irreversible oxidation of hemoglobin in erythrocytes. Iron from the intestines controls its absorption [3].

2. GLUTATHIONE SYNTHESIS

GSH is abundantly (0.5–10 mM) synthesized in all mammalian cells. This synthesis consists of two sequential steps. GSH produces the enzyme γ-glutaminecysteine synthetase in the first step. It catalyzes the formation of γ-glutaminecysteine from glutamate and cysteine, its precursor amino acids. Glutathione synthetase then converts glycine and γ-glutamine cysteine into glutathione in the second step. In this synthesis, hydrolysis of 2 molecules of ATP is required for 1 molecule of GSH. [10, 11] (Fig. 3).

ISBN: 978-625-6971-51-6

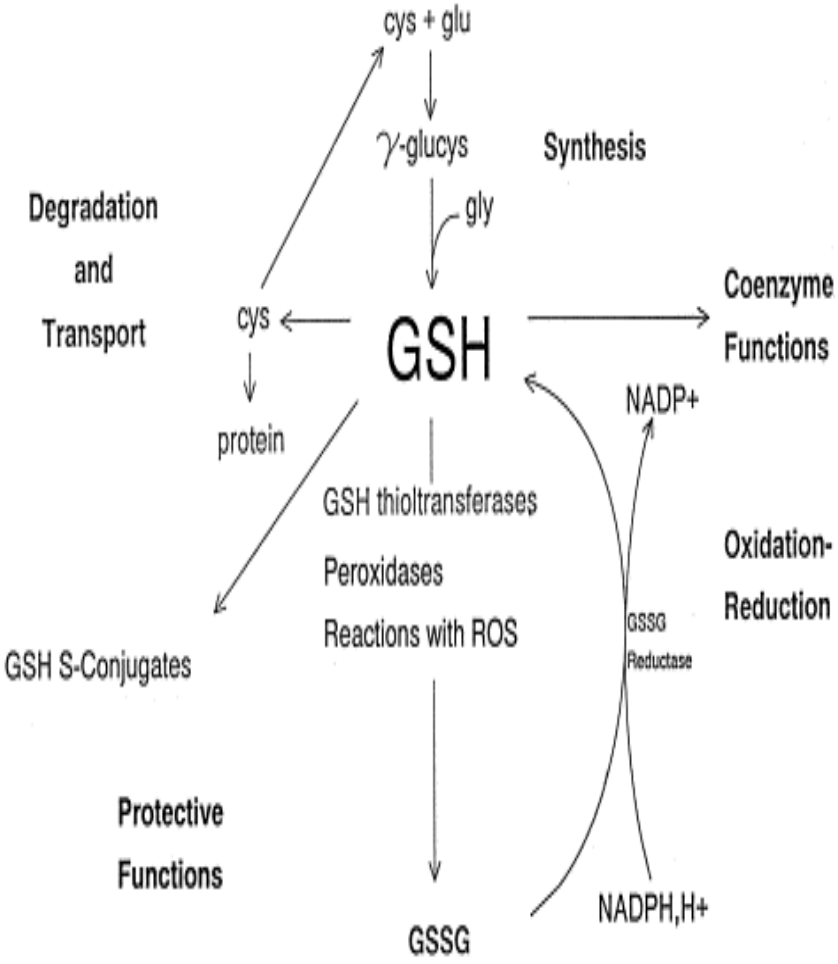


Figure 3. Formation and other mechanisms of glutathione [12].

3. THE ROLE OF GLUTATHIONE IN METABOLISM

Glutathione is responsible for DNA and protein synthesis and the regulation of enzyme activities. In addition, glutathione has cellular functions such as intra- and extracellular transports. One of its most important functions is to act as an antioxidant substance. Glutathione is essential for cellular functions and protects the brain, heart, and immune system cells, as well as the kidney, eye, liver, lung, and skin tissues against oxidative damage. It has an anti-aging effect [1, 13, 14].

Glutathione (GSH) in cells, tissues, and organs helps to maintain system structural and functional integrity. Its role as an antioxidant molecule in the preserva-

tion of is significant. GSH is important in terms of its involvement in the pathophysiology of many diseases, such as cancer, aging, atherosclerosis, and neurodegenerative diseases [15].

GSH also subjects cells to oxidative stress, toxic chemicals, and radiation. Some endogenous drugs, such as estrogen, prostaglandin, and leukotrienes, take part in the metabolic processes of compounds [14, 16–18].

GSH is very important for organs such as the lungs, intestines, kidneys, and partly the liver. Because these organs can be exposed to exogenous toxins. GSH plays an important role in the elimination of toxins [19, 20]. GSH in the lungs regulates the development of inflammation and oxidative/nitrosative stress. It acts as an intracellular and extracellular protective antioxidant against stress [21].

Chronic viral infections trigger circulating immune system cells to consume GSH. GSH is required for cell proliferation, growth, and differentiation. In patients with acute and chronic viral hepatitis, low GSH concentrations were detected in erythrocytes [22]. In another study, a decrease in GSH was seen in the plasma of patients with chronic liver disease. It has also been reported that the levels of trace elements such as Fe, Zn, and Se are significantly reduced [23].

The brain is an oxygenated tissue with a high concentration of free unsaturated fatty acids, making it vulnerable to oxidative damage. GSH, as both a redox modulator and an antioxidant, plays an important role in the nervous system. Various studies have shown that the brains of Parkinson's patients have increased metal levels, low GSH, and high lipid peroxidation compared to control groups [24, 25]. GSH and GSSG levels, which form the main thiol redox system of the cell, are affected by nutrition, drugs, and oxidative stress [26]. The effect causes a significant change. As the GSH level decreases, the oxidized glutathione (GSSG) level will increase. For this reason, the GSH/GSSG balance in metabolism is disturbed. Maintaining the GSH/GSSG ratio is important for its sustainability [27]. Multiple enzyme systems, including -glutamyl transpeptidase, amino acid transporters, glutathione peroxidase, and glutathione reductase, keep the cellular level of GSH stable. [28]. When the cell is exposed to a high amount of oxidant, GSSG formation metabolically exceeds the limit, and oxidative stress occurs [29, 30].

ISBN: 978-625-6971-51-6

$$\mathbf{ROOH + 2GSH \xrightarrow{GSH\text{-}Px} ROH + GSSG} \quad \mathbf{(1)}$$

$$\mathbf{HOOH + 2\ GSH \xrightarrow{GSH\text{-}Px} 2H2O + GSSG} \quad \mathbf{(2)}$$

$$\mathbf{GSSG + NADPH + H^{+} \xrightarrow{GSH\text{-}Rd} 2\ GSH + NADP^{+}} \quad \mathbf{(3)}$$

Glutathione plays an important role in the uptake of oxygen by plants [31]. End in the studies carried out over the years, the reactive oxygen products (ROS) of various stress models have been determined. has been reported to accelerate its formation. Free oxygen species also cause lipid peroxidation [30, 32]. Oxidative damage caused by ROS is defined as "oxidant stress." It is known that GSH levels decrease during oxidative stress [33, 34].

Substances that inactivate oxidants are called antioxidants. In healthy people, free radicals/antioxidants are in equilibrium. In diabetes, this balance deteriorates in favor of free radicals [35, 36]. Glutathione (GSH) has important roles in providing structural and functional functions of cells, tissues, and organs. It can fulfill this task as an antioxidant molecule. With excessive oxidative stress or an antioxidant deficiency, the level of GSH decreases. Therefore, pathological conditions arise in metabolism As a result of its deficiency, cell damage occurs in many tissues [15]. In the metabolism, glutathione acts as an antioxidant. Moreover, it is responsible for maintaining the redox state of the cell. Glutathione is one of the antioxidants in metabolism [37].

4. REFERENCES

[1] Meister, A., Anderson, M.E. (1983). Glutathione. Ann Rev Biochem, 52: 711-760.

[2] Meister, A. (1994). Glutathione, ascorbate and cellular protection. Cancer Res Suppl, 954: 1969-1975.

[3] Ası, T. (1996). 'Tablolarda Biyokimya', cilt 1, syf : 222.

[4] Gözükara, E. (2001). "Biyokimya", cilt 1, syf : 709-712.

[5] Akkuş, İ. (1995). Serbest radikaller ve fizyopatolojik etkileri. Mimoza Yayınları, Konya-Türkiye.

[6] Townsend, D.M., Tew, K.D., Tapiero, H. (2003). The importance of glutathione in human disease. Biomed Pharmacother. 57 (3-4): 145- 155.

[7] Green, R.M., Graham, M., O'Donovan, M.R., Chipman, J.K., Hodges, N.J. (2006). Subcellular compartmentalization of glutathione: correlations with parameters of oxidative stress related to genotoxicity. Mutagenesis. 21 (6): 383-390.

[8] Kalinina, E.V., Chernov, N.N., Novichkova, M.D. (2014). Role of Glutathione, Glutathione Transferase, and Glutaredoxin in Regulation of Redox-Dependent Processes. Published in Uspekhi Biologicheskoi Khimii. 54: 299-348.

[9] Emerk, K., Onat, T. (1997). Temel biyokimya, 2. Baskı, Saray Medikal Yayıncılık ve Tic.Ltd.Sti, İzmir-Türkiye.

[10] Mutoh, H., Hiraishi, H., Ota, S., Yoshida, H., Ivey, K.J., Terano, A., Sugimoto, T. (1990). Protective role of intracellular glutathione against ethanol-induced damage in cultured rat gastric mucosal cells. Gastroenterology, 98 (6): 1452-1459.

[11] Cochrane, C.G. (1991). Cellular injury by oxidants. Am J Med, 3C23S-3C30S.

[12] Anderson, M.E. (1998). Glutathione: an overview of biosynthesis and modulation. Chemico-Biological Interactions, 111-112: 1-14.

[13] Deneke, S.M., Fanburg, B.L. (1989). Regulation of cellular glutathione. Am J Physiol, 257: L163-L173.

[14] Meister, A. (1983). Selective modification of glutathione metabolism. Science, 220: 472-477.

[15] Aksoy, Y. (2002). The role of Glutathione in antioxidant mechanism. T Klin J Med Sci, 22: 442-448.

[16] Meister, A. (1991). Glutathione Deficiency Produced by Inhibition of Its Synthesis, and Its Reversal; Application in Research and Therapy. Pharmacol Ther, 51: 155-85.

[17] Meister A. (1985). Methods for selective modification of Glutathione Metabolism and Study of Glutathione Transport. Methods Enzymol, 113: 571-85.

[18] Meister, A. (1988). Glutathione Metabolism and its Selective

Modification. J Biol Chem, 263: 17205-17208.

[19] Lomaestro, B.M., Malone, M. (1995). Glutathione in health and disease: Pharmacotherapeutic Issues. Annals Pharmacother, 29: 1263-1273.

[20] Anderson, M.E. (1985). Determination of Glutathione and Glutathione Disulphide in Biological Samples. Methods in Enzymology, 113: 548-555.

[21] Rahman, I., MacNee, W. (2000). Oxidative Stress and Regulation of Glutathione in Lung Inflammation. Eur Respir J., 16: 534-554.

[22] Swietek, K., Juszczyk, J. (1997). Reduced Glutathione Concentration in Erythrocytes of Patients with Acute and Chronic Viral Hepatitis. J Viral Hepat, 4: 139-141.

[23] Loguercio, C., De Girolamov, V., Federico, A., Feng, S.L., Crafa, E., Cataldi, V., Gialanella, G., Moro, R., Del Vecchio Blanco, C. (2001). Relationship of Blood Trace Elements to Liver Damage, Nutritional Status and Oxidative Stress in Chronic Nonalcoholic Liver Diseases. Biol.Trace Elem Res, 81: 245-54.

[24] Han, J., Cheng, F.C., Yang, Z., Dryhurst, G. (1999). Inhibitors of Mitochondrial Respiration, Iron (II) and Hydroxyl Radical Evoke Release and Extracellular Hydrolysis of Glutathione in Rat Striatum and Substantia Nigra: Potential Implications to Parkinson's Disease. J Neurochem, 73: 1683-1695.

[25] Merad-Boudia, M., Nicole, A., Santiard-Baron, D., Saillé, C., Ceballos-Picot, I. (1998). Mitochondrial Impairment as an Early Event in the Process of Apoptosis Induced by Glutathione Depletion in Neuronal Cells: Relevance to Parkinson's Disease. Biochem Pharmacol, 56: 645-655.

[26] Seppi, C., Castellana, M.A., Minetti, G., Piccinini, G., Balduini, C., Brovelli, A. (1991). Evidence for Membrane Protein Oxidation During in Vivo Aging of Human Erythrocytes. Mech Ageing Dev, 57: 247-258.

[27] Mieyal, J.J., Starke, D.W., Gravina, A., Dothey, C., Chung, J.S. (1991). Thioltransferase in Human Red Blood Cells: Purification and properties. Biochemistry, 30: 6088-6097.

[28] Cnubben, N.H.P., Rietjens, I.M.C.M., Wortelboer, H., Zanden, J., Bladeren, P.J. (2001). The interplay of glutathione-related processes in antioxidant defense. Environmental Toxicology and Pharmacology.10: 141-152.

[29] Ambrosio, G., Santoro, G., Tritto, I., Elia, P.P., Duilio, C., Basso, A., Scoqnamiqlio, A., Chiariello, M. (1992). Effects of ischemia and reperfusion on cardiac tolerance to oxidative stress. Am J Physiol, 262: H23-H30.

[30] Goldin, E., Ardite, E., Elizalde, J.I., Odriozola, A., Panés, J., Piqué, J.M., Fernández-Checa, J.C. (1997). Gastric mucosal damage in experimental diabetes in rats: role of endogenous glutathione. Gastroenterology, 112: 855- 863.

[31] Gözükara, E. (2001). "Biyokimya", cilt 1, sf : 709-712.

[32] Das, D., Banerjee, R.K. (1993). Effect of stress on the antioxidant enzymes and gastric ulceration. Mol Cell Biochem, 125: 115-125.

[33] Menguy, R. (1981). Role of gastric mucosal energy metabolism in the etiology of stress ulceration. World J Surg, 5: 175-180.

[34] Pal, S.N., Dandiya, P.C. (1994). Glutathione as a cerebral substrate in depressive behavior. Pharmacol Biochem Behav, 48: 845-851.

[35] Memisogullari, R., Taysi, S., Bakan, E., Capoglu, I. (2003). Antioxidant Status and Lipid Peroxidation in Type II Diabetes Mellitus. Cell Biochem Func, 21: 291-296.

[36] Memisoğulları, R., Bakan, E. (2004). Levels of ceruloplasmin, transferrin, and lipid peroxidation in the serum of patients with Type 2 diabetes mellitus. Journal of Diabetes and Its Complications. 18: 193– 197.

[37] Townsend, D.M., Tew, K.D., Tapiero, H. (2003). The importance of glutathione in human disease. Biomed Pharmacother, 57 (3-4): 145- 155.

ISBN: 978-625-6971-51-6


CHAPTER
5

ISBN: 978-625-6971-51-6

MANIPULATION OF GUT MICROBIOTA BACTERIA FOR THERAPEUTIC PURPOSES

Assist. Prof. Taha CEYLANI, Ph.D
Department of Molecular Biology and Genetics
Muş Alparslan University
ORICID: 0000-0002-3041-6010

1. Introduction

The human gut harbors a complex and diverse community of microorganisms, collectively known as the gut microbiota (Tremaroli and Bäckhed, 2012). Recent advances in sequencing technologies and bioinformatics have enabled the comprehensive analysis of gut microbiota composition and function, revealing their crucial role in host health and disease (Fomby and Cherlin, 2011; Sender et al., 2016). Dysbiosis, defined as an imbalance in gut microbiota composition and function, has been associated with a range of diseases, including inflammatory bowel disease, obesity, and type 2 diabetes (Lloyd-Price et al., 2016; Wang et al., 2012).

Manipulation of gut microbiota has emerged as a promising therapeutic strategy for a range of diseases. Several approaches have been developed to target specific bacterial species or functional pathways within the gut microbiota, including prebiotics, probiotics, antibiotics, and fecal microbiota transplantation (Bäckhed et al., 2012; Kelly et al., 2015). However, the efficacy and safety of these approaches vary widely, and further research is needed to develop targeted and personalized microbiota-based therapies (Nieuwdorp et al., 2014).

In this chapter, we discuss the current understanding of gut microbiota composition and function, as well as the strategies for manipulation of gut microbiota bacteria for therapeutic purposes. We also highlight the potential applications of gut microbiota manipulation and the challenges and future directions in this field.

2. Gut Microbiota and Health

The gut microbiota performs a range of important functions that are essential for host health. These include the production of vitamins, metabolism of dietary nutrients, and protection against pathogens (Nicholson et al., 2012). In addition, the gut microbiota plays a crucial role in the development and function of the host immune system, with recent evidence suggesting that the gut microbiota is involved in the regulation of immune responses both locally in the gut and systemically throughout the body (Fomby and Cherlin, 2011; Honda and Littman, 2016).

Disruptions to gut microbiota composition and function, referred to as dysbiosis, have been linked to a range of diseases, including inflammatory bowel disease (IBD), obesity, and type 2 diabetes (Longo et al., 2021; Wang et al., 2012). For example, patients with IBD have been found to have a lower diversity of gut microbiota and a higher abundance of potentially pathogenic bacteria, suggesting a role for dysbiosis in the development and progression of the disease (Frank et al., 2007). Similarly, studies have shown that the gut microbiota of obese individuals is different from that of lean individuals, with changes in the abundance of specific bacterial species associated with obesity-related metabolic disorders (Turnbaugh et al., 2006).

Given the important role of gut microbiota in health and disease, strategies aimed at manipulation of gut microbiota have been developed for therapeutic purposes. These approaches include prebiotics, probiotics, antibiotics, and fecal microbiota transplantation, among others (Bäckhed et al., 2012). While these approaches have shown promise in some cases, their efficacy and safety are still being investigated, and further research is needed to develop targeted and personalized microbiota-based therapies.

3. Manipulation of Gut Microbiota

Manipulation of gut microbiota has emerged as a promising therapeutic strategy for a range of diseases (Haiser and Turnbaugh, 2013). Several approaches have been developed to target specific bacterial species or functional pathways within the gut microbiota, including prebiotics, probiotics, antibiotics, and fecal microbiota transplantation (Bäckhed et al., 2015; Kelly et al., 2015).

Prebiotics are non-digestible food components that selectively stimulate the growth and activity of beneficial bacteria in the gut, such as bifidobacteria and lactobacilli (Gibson et al., 2017). These compounds include fructooligosaccharides, inulin, and galactooligosaccharides, among others, and are commonly

found in fruits, vegetables, and grains. Prebiotics have been shown to have beneficial effects on gut microbiota composition and function, as well as on host health outcomes (Roberfroid et al., 2010).

Probiotics, on the other hand, are live microorganisms that, when administered in adequate amounts, confer a health benefit on the host (Hill et al., 2014). These include various bacterial strains, such as *Lactobacillus* and *Bifidobacterium*, and yeast strains, such as *Saccharomyces boulardii*. Probiotics have been shown to have beneficial effects on gut microbiota composition and function, as well as on host immune function, gut barrier function, and digestive health (Hill et al., 2014; Sanders et al., 2016).

Antibiotics are commonly used to treat bacterial infections, but they can also have unintended effects on gut microbiota composition and function (Langdon et al., 2016). Antibiotics can lead to dysbiosis, with reductions in beneficial bacterial species and increases in potentially pathogenic species. This can lead to a range of negative health outcomes, such as increased risk of infection, inflammation, and metabolic disorders (Vangay et al., 2015).

Fecal microbiota transplantation (FMT) involves the transfer of fecal material from a healthy donor to the gastrointestinal tract of a recipient, with the goal of restoring a healthy gut microbiota (Kelly et al., 2012). FMT has been shown to be highly effective in the treatment of recurrent *Clostridium difficile* infection, and is being investigated as a potential therapy for a range of other diseases, including inflammatory bowel disease, metabolic disorders, and neurodegenerative diseases (Kassam et al., 2013; Saha et al., 2019).

In addition to these approaches, other strategies for manipulation of gut microbiota are also being investigated, including postbiotics, which are metabolites produced by probiotic bacteria, and microbial biotherapeutics, which involve the use of genetically engineered or synthetic bacteria for therapeutic purposes (Ilhan et al., 2017; Lebeer et al., 2010). These approaches have the potential to provide targeted and personalized therapies for a range of diseases, but further research is needed to fully understand their efficacy and safety.

4. Strategies for Targeted Bacterial Manipulation

Targeted manipulation of specific bacterial species or functional pathways within the gut microbiota can be achieved through a range of strategies, including dietary interventions, use of specific bacterial strains, and bacteriophages (Barr et al., 2013; Sonnenburg and Sonnenburg, 2014).

Dietary interventions can be used to selectively stimulate the growth of specific bacterial species or functional pathways within the gut microbiota. For example, a diet high in fiber has been shown to promote the growth of *Bifidobacterium* and other beneficial bacteria in the gut, while reducing the abundance of potentially pathogenic species (De Filippis et al., 2016). Similarly, consumption of polyphenols, found in fruits, vegetables, and beverages such as tea and wine, has been shown to have beneficial effects on gut microbiota composition and function, through their prebiotic and antimicrobial properties (Selma et al., 2009).

Specific bacterial strains can also be used for targeted manipulation of gut microbiota. For example, the probiotic strain *Lactobacillus rhamnosus* GG has been shown to have beneficial effects on gut microbiota composition and function, and is used clinically for the prevention and treatment of a range of gastrointestinal disorders (Salminen et al., 1998). Other bacterial strains, such as *Faecalibacterium prausnitzii* and *Akkermansia muciniphila*, have also been shown to have beneficial effects on gut microbiota composition and function, and are being investigated as potential probiotic strains (Derrien et al., 2008; Sokol et al., 2008).

Bacteriophages, or viruses that infect and replicate within bacterial cells, can also be used for targeted manipulation of gut microbiota. Bacteriophages can be used to selectively eliminate specific bacterial species within the gut microbiota, without affecting other beneficial bacterial species (Barr et al., 2015). Bacteriophages have been shown to be effective in the treatment of bacterial infections, and are being investigated as a potential therapy for dysbiosis-related diseases (Dąbrowska, 2019).

These strategies have the potential to provide targeted and personalized therapies for a range of diseases associated with dysbiosis. However, further research is needed to fully understand their efficacy and safety, as well as the mechanisms underlying their effects on gut microbiota composition and function.

5. Advancements in Microbiota-Based Therapies

Microbiota-based therapies are a rapidly developing area of research, with advancements in the understanding of gut microbiota composition and function driving the development of new therapies (Gilbert et al., 2018). Some of the latest advancements in microbiota-based therapies include the following:

Precision microbiome engineering: This involves the use of synthetic biology to engineer bacterial strains with specific functions, such as the production of therapeutic compounds or the elimination of pathogenic bacteria (Riglar et al., 2017).

ISBN: 978-625-6971-51-6

Microbiota transplantation from elite athletes: Recent research has shown that transplantation of fecal microbiota from elite athletes to sedentary individuals can lead to improvements in exercise performance and metabolic health(Scheiman et al., 2019).

Microbiota-derived metabolites: Metabolites produced by gut bacteria, such as short-chain fatty acids and secondary bile acids, have been shown to have beneficial effects on host health, including modulation of the immune system and regulation of host metabolism. Researchers are investigating the therapeutic potential of these metabolites for the treatment of a range of diseases, including inflammatory bowel disease and metabolic disorders (Canfora et al., 2019; Ridlon et al., 2006).

Host-microbiota crosstalk: Advances in understanding of host-microbiota crosstalk have revealed the complex interplay between gut microbiota and host physiology. Researchers are investigating the mechanisms underlying this crosstalk, with the goal of developing targeted therapies that manipulate these interactions for therapeutic benefit (Fomby and Cherlin, 2011).

Microbiota-targeted therapies: Novel approaches for microbiota-targeted therapies are being developed, including selective targeting of specific bacterial species or functional pathways within the gut microbiota, as well as targeted delivery of therapeutic compounds to the gut microbiota (Feng et al., 2020).

These advancements have the potential to revolutionize the treatment of a range of diseases associated with dysbiosis, including inflammatory bowel disease, metabolic disorders, and neurodegenerative diseases. However, further research is needed to fully understand the mechanisms underlying these therapies, as well as their efficacy and safety in clinical settings.

6. Potential Applications of Gut Microbiota Manipulation

Manipulation of the gut microbiota has the potential to be applied to a range of diseases and disorders associated with dysbiosis. Some potential applications include:

Inflammatory bowel disease (IBD): Dysbiosis has been implicated in the pathogenesis of IBD, and microbiota-based therapies have shown promise in the treatment of IBD, including fecal microbiota transplantation (FMT) and use of specific bacterial strains (Eindor-Abarbanel et al., 2021).

Obesity and metabolic disorders: Dysbiosis has been associated with obesity and metabolic disorders, and microbiota-based therapies, including use of specific bacterial strains and prebiotics, have shown potential in the treatment of these conditions (Bouter et al., 2017; Dao et al., 2016)(2,3).

Neurodegenerative diseases: Dysbiosis has been linked to neurodegenerative diseases, including Parkinson's disease and Alzheimer's disease, and microbiota-based therapies have shown promise in preclinical studies (Bonfili et al., 2017; Sampson et al., 2016)(4,5).

Mood disorders: Dysbiosis has been implicated in mood disorders, including depression and anxiety, and microbiota-based therapies, including use of specific bacterial strains and FMT, have shown promise in preclinical studies (Foster et al., 2017; Kelly et al., 2016)(6,7).

Cancer: Dysbiosis has been implicated in the pathogenesis of certain types of cancer, and microbiota-based therapies have shown potential in cancer prevention and treatment (Manuscript, 2012; Viaud et al., 2015). Recent studies have demonstrated the potential for microbiota-based therapies in cancer treatment, particularly in combination with immunotherapy. The gut microbiome has been found to influence the efficacy of anti-PD-1-based immunotherapy against epithelial tumors, with commensal microbiota associated with improved treatment outcomes (Matson et al., 2018; Santoni et al., 2018). Additionally, gut microbiome modulation has been shown to enhance response to anti-PD-1 immunotherapy in melanoma patients (Biphenyls, 2015). Fecal microbiota transplantation has also shown promise in the treatment of refractory immune checkpoint inhibitor-associated colitis (Wang et al., 2018).

These potential applications demonstrate the wide-ranging therapeutic potential of gut microbiota manipulation, and highlight the need for further research to fully understand the mechanisms underlying these therapies, as well as their efficacy and safety in clinical settings.

7. Challenges and Future Directions

While the potential for gut microbiota manipulation as a therapeutic approach is exciting, there are also significant challenges that must be addressed before these therapies can be widely applied in clinical settings. Some of the key challenges and future directions include:

Safety and efficacy: The safety and efficacy of microbiota-based therapies must be rigorously evaluated in clinical trials, with a focus on long-term safety and efficacy, as well as potential side effects and adverse events.

ISBN: 978-625-6971-51-6

Personalized approaches: Gut microbiota composition and function are highly variable between individuals, and personalized approaches to gut microbiota manipulation may be necessary for optimal therapeutic outcomes. This will require the development of tools for rapid and accurate assessment of gut microbiota composition and function, as well as the ability to predict individual responses to specific microbiota-based therapies.

Mechanistic understanding: A better understanding of the mechanisms underlying the effects of gut microbiota manipulation is necessary for the development of targeted and effective therapies. This will require a combination of experimental and computational approaches to unravel the complex interactions between gut microbiota and host physiology.

Regulatory challenges: Microbiota-based therapies are subject to regulatory challenges, including classification as drugs or biologics, and the need for rigorous safety and efficacy evaluation. The regulatory framework for these therapies will need to be developed to ensure patient safety and access to effective therapies.

Commercialization: The commercialization of microbiota-based therapies presents unique challenges, including the need for large-scale production of specific bacterial strains, and the development of sustainable business models for these therapies.

Addressing these challenges and advancing our understanding of gut microbiota composition and function will be critical for the successful development and implementation of microbiota-based therapies for a range of diseases and disorders associated with dysbiosis.

Overall, the field of gut microbiota manipulation is rapidly evolving, with exciting developments and potential applications emerging. While there are significant challenges that must be addressed, the potential for microbiota-based therapies to transform the treatment of a range of diseases and disorders is immense, and warrants continued research and investment.

8. Conclusion and Future Outlook

The gut microbiota is a complex and dynamic ecosystem that plays a critical role in human health and disease. Dysbiosis, or disruption of gut microbiota composition and function, has been implicated in the pathogenesis of a range of diseases and disorders, including inflammatory bowel disease, obesity, neurodegenerative diseases, and mood disorders. Manipulation of the gut microbiota has

emerged as a promising approach for the treatment of these conditions, with potential applications including the use of specific bacterial strains, fecal microbiota transplantation, and microbiota-derived metabolites.

While the field of gut microbiota manipulation is still in its infancy, recent advancements in our understanding of gut microbiota composition and function, as well as new technologies for precision microbiome engineering and microbiota-based therapies, offer exciting opportunities for the development of novel and effective treatments for a range of diseases and disorders.

However, significant challenges must be addressed, including the need for rigorous evaluation of safety and efficacy, the development of personalized approaches to gut microbiota manipulation, and the need for a better mechanistic understanding of the effects of gut microbiota manipulation.

In conclusion, the gut microbiota represents a promising target for the development of novel and effective therapies for a range of diseases and disorders associated with dysbiosis. Further research and investment in this field are needed to fully realize the potential of microbiota-based therapies, and to ensure that these therapies are safe, effective, and accessible to patients in need.

ISBN: 978-625-6971-51-6

References

Bäckhed, F., Fraser, C.M., Ringel, Y., Sanders, M.E., Sartor, R.B., Sherman, P.M., Versalovic, J., Young, V., Finlay, B.B., 2012. Defining a healthy human gut microbiome: Current concepts, future directions, and clinical applications. Cell Host Microbe 12, 611–622. https://doi.org/10.1016/j.chom.2012.10.012

Bäckhed, F., Roswall, J., Peng, Y., Feng, Q., Jia, H., Kovatcheva-Datchary, P., Li, Y., Xia, Y., Xie, H., Zhong, H., Khan, M.T., Zhang, J., Li, J., Xiao, L., Al-Aama, J., Zhang, D., Lee, Y.S., Kotowska, D., Colding, C., Tremaroli, V., Yin, Y., Bergman, S., Xu, X., Madsen, L., Kristiansen, K., Dahlgren, J., Jun, W., 2015. Dynamics and stabilization of the human gut microbiome during the first year of life. Cell Host Microbe 17, 690–703. https://doi. org/10.1016/j.chom .2015.04.004

Barr, J.J., Auro, R., Furlan, M., Whiteson, K.L., Erb, M.L., Pogliano, J., Stotland, A., Wolkowicz, R., Cutting, A.S., Doran, K.S., Salamon, P., Youle, M., Rohwer, F., 2013. Bacteriophage adhering to mucus provide a non-host-derived immunity. Proc. Natl. Acad. Sci. U. S. A. 110, 10771–10776. https://doi.org/10.1073/pnas.1305923110

Barr, J.J., Auro, R., Sam-Soon, N., Kassegne, S., Peters, G., Bonilla, N., Hatay, M., Mourtada, S., Bailey, B., Youle, M., Felts, B., Baljon, A., Nulton, J., Salamon, P., Rohwer, F., 2015. Subdiffusive motion of bacteriophage in mucosal surfaces increases the frequency of bacterial encounters. Proc. Natl. Acad. Sci. U. S. A. 112, 13675–13680. https://doi.org/10.1073/pnas.1508355112

Biphenyls, C.P., 2015. Gut microbiome modulates response to anti–PD-1 immunotherapy in melanoma patients 91, 165–171. https://doi.org/10. 1016/j.chemosphere.2012.12.037.Reactivity

Bonfili, L., Cecarini, V., Berardi, S., Scarpona, S., Suchodolski, J.S., Nasuti, C., Fiorini, D., Boarelli, M.C., Rossi, G., Eleuteri, A.M., 2017. Microbiota modulation counteracts Alzheimer's disease progression influencing neuronal proteolysis and gut hormones plasma levels. Sci. Rep. 7, 1–21. https://doi. org/10.1038/s41598-017-02587-2

Bouter, K.E., van Raalte, D.H., Groen, A.K., Nieuwdorp, M., 2017. Role of the Gut Microbiome in the Pathogenesis of Obesity and Obesity-Related Metabolic Dysfunction. Gastroenterology 152, 1671–1678. https://doi.org/10.1053/j.gastro.2016.12.048

Canfora, E.E., Meex, R.C.R., Venema, K., Blaak, E.E., 2019. Gut microbial metabolites in obesity, NAFLD and T2DM. Nat. Rev. Endocrinol. 15, 261–273. https://doi.org/10.1038/s41574-019-0156-z

Dąbrowska, K., 2019. Phage therapy: What factors shape phage pharmacokinetics and bioavailability? Systematic and critical review. Med. Res. Rev. 39, 2000–2025. https://doi.org/10.1002/med.21572

Dao, M.C., Everard, A., Aron-Wisnewsky, J., Sokolovska, N., Prifti, E., Verger, E.O., Kayser, B.D., Levenez, F., Chilloux, J., Hoyles, L., Dumas, M.E., Rizkalla, S.W., Doré, J., Cani, P.D., Clément, K., Le Mouhaër, S., Cotillard, A., Kennedy, S.P., Pons, N., Le Chatelier, E., Almeida, M., Quinquis, B., Galleron, N., Batto, J.M., Renault, P., Zucker, J.D., Ehrlich, S.D., Blottière, H., Leclerc, M., Juste, C., De Wouters, T., Lepage, P., 2016. Akkermansia muciniphila and improved metabolic health during a dietary intervention in obesity: Relationship with gut microbiome richness and ecology. Gut 65, 426–436. https://doi.org/10.1136/gutjnl-2014-308778

De Filippis, F., Pellegrini, N., Vannini, L., Jeffery, I.B., La Storia, A., Laghi, L., I Serrazanetti, D., Di Cagno, R., Ferrocino, I., Lazzi, C., Turroni, S., Cocolin, L., Brigidi, P., Neviani, E., Gobbetti, M., O'Toole, P.W., Ercolini, D., 2016. High-level adherence to a Mediterranean diet beneficially impacts the gut microbiota and associated metabolome. Gut 65, 1–10. https://doi.org/10.1136/gutjnl-2015-309957

Derrien, M., Collado, M.C., Ben-Amor, K., Salminen, S., De Vos, W.M., 2008. The mucin degrader Akkermansia muciniphila is an abundant resident of the human intestinal tract. Appl. Environ. Microbiol. 74, 1646–1648. https://doi.org/10.1128/AEM.01226-07

Eindor-Abarbanel, A., Healey, G.R., Jacobson, K., 2021. Therapeutic advances in gut microbiome modulation in patients with inflammatory bowel disease from pediatrics to adulthood. Int. J. Mol. Sci. 22. https://doi. org/10.3390/ijms222212506

Feng, W., Liu, J., Ao, H., Yue, S., Peng, C., 2020. Targeting gut microbiota for precision medicine: Focusing on the efficacy and toxicity of drugs. Theranostics 10, 11278–11301. https://doi.org/10.7150/thno.47289

Fomby, P., Cherlin, A.J., 2011. Role of microbiota in immunity and inflammation. Natl. Inst. Heal. 72, 181–204. https://doi. org/10.1016/j.cell.2014.03.011.Role

Foster, J.A., Rinaman, L., Cryan, J.F., 2017. Stress & the gut-brain axis: Regulation by the microbiome. Neurobiol. Stress 7, 124–136. https://doi.org/10.1016/j.ynstr.2017.03.001

Frank, D.N., St. Amand, A.L., Feldman, R.A., Boedeker, E.C., Harpaz, N., Pace, N.R., 2007. Molecular-phylogenetic characterization of microbial community imbalances in human inflammatory bowel diseases. Proc. Natl. Acad. Sci. U. S. A. 104, 13780–13785. https://doi.org/10.1073/pnas.0706625104

Gibson, G.R., Hutkins, R., Sanders, M.E., Prescott, S.L., Reimer, R.A., Salminen, S.J., Scott, K., Stanton, C., Swanson, K.S., Cani, P.D., Verbeke, K., Reid, G., 2017. Expert consensus document: The International Scientific Association for Probiotics and Prebiotics (ISAPP) consensus statement on the definition and scope of prebiotics. Nat. Rev. Gastroenterol. Hepatol. 14, 491–502. https://doi.org/10.1038/nrgastro.2017.75

Gilbert, J.A., Blaser, M.J., Caporaso, J.G., Jansson, J.K., Lynch, S. V., Knight, R., 2018. Current understanding of the human microbiome. Nat. Med. 24, 392–400. https://doi.org/10.1038/nm.4517

Haiser, H.J., Turnbaugh, P.J., 2013. Developing a metagenomic view of xenobiotic metabolism. Pharmacol. Res. 69, 21–31. https://doi.org/10.1016/j.phrs.2012.07.009

Hill, C., Guarner, F., Reid, G., Gibson, G.R., Merenstein, D.J., Pot, B., Morelli, L., Canani, R.B., Flint, H.J., Salminen, S., Calder, P.C., Sanders, M.E., 2014. Expert consensus document: The international scientific association for probiotics and prebiotics consensus statement on the scope and appropriate use of the term probiotic. Nat. Rev. Gastroenterol. Hepatol. 11, 506–514. https://doi.org/10.1038/nrgastro.2014.66

Honda, K., Littman, D.R., 2016. The microbiota in adaptive immune homeostasis and disease. Nature 535, 75–84. https://doi.org/10.1038/nature18848

Ilhan, Z.E., Marcus, A.K., Kang, D., Rittmann, B.E., 2017. pH-Mediated Microbial and Metabolic. mSphere 2, 1–12.

Kassam, Z., Lee, C.H., Yuan, Y., Hunt, R.H., 2013. Fecal microbiota transplantation for clostridium difficile infection: Systematic review and meta-analysis. Am. J. Gastroenterol. 108, 500–508. https://doi.org/10.1038/ajg.2013.59

Kelly, C.R., De Leon, L., Jasutkar, N., 2012. Fecal microbiota transplantation for relapsing clostridium difficile infection in 26 patients: Methodology and results. J. Clin. Gastroenterol. 46, 145–149. https://doi.org/10.1097/MCG.0b013e318234570b

Kelly, C.R., Kahn, S., Kashyap, P., Laine, L., Rubin, D., Atreja, A., Applab, S., Moore, T., Wu, G., 2015. Update on FMT 2015: Indications, Methodologies, Mechanisms and Outlook Members of the Steering Committee for the AGA FMT Registry HHS Public Access. Gastroenterology 149, 223–237. https://doi.org/10.1053/j.gastro.2015.05.008.Update

Kelly, J.R., Borre, Y., O' Brien, C., Patterson, E., El Aidy, S., Deane, J.,

Kennedy, P.J., Beers, S., Scott, K., Moloney, G., Hoban, A.E., Scott, L., Fitzgerald, P., Ross, P., Stanton, C., Clarke, G., Cryan, J.F., Dinan, T.G., 2016. Transferring the blues: Depression-associated gut microbiota induces neurobehavioural changes in the rat. J. Psychiatr. Res. 82, 109–118. https://doi.org/10.1016/j.jpsychires.2016.07.019

Langdon, A., Crook, N., Dantas, G., 2016. The effects of antibiotics on the microbiome throughout development and alternative approaches for therapeutic modulation. Genome Med. https: // doi. org/10. 1186/s13073-016- 0294-z

Lebeer, S., Vanderleyden, J., De Keersmaecker, S.C.J., 2010. Host interactions of probiotic bacterial surface molecules: Comparison with commensals and pathogens. Nat. Rev. Microbiol. 8, 171–184. https://doi.org/10.1038/nrmicro2297

Lloyd-Price, J., Abu-Ali, G., Huttenhower, C., 2016. The healthy human microbiome. Genome Med. 8, 51. https://doi.org/10.1186/s13073-016-0307-y

Longo, V.D., Di Tano, M., Mattson, M.P., Guidi, N., 2021. Intermittent and periodic fasting, longevity and disease. Nat. aging 1, 47–59. https://doi.org/10.1038/s43587-020-00013-3

Manuscript, A., 2012. The microbiome and cancer Robert. Changes 29, 997–1003. https://doi. org/10. 1038/nrc3610.The

Matson, V., Fessler, J., Bao, R., Chongsuwat, T., Zha, Y., Alegre, M.L., Luke, J.J., Gajewski, T.F., 2018. The commensal microbiome is associated with anti-PD-1 efficacy in metastatic melanoma patients. Science (80-.). 359, 104–108. https://doi.org/10.1126/science.aao3290

Nicholson, J.K., Holmes, E., Kinross, J.M., Darzi, A.W., Takats, Z., Lindon, J.C., 2012. Metabolic phenotyping in clinical and surgical environments. Nature 491, 384–392. https://doi.org/10.1038/nature11708

Nieuwdorp, M., Gilijamse, P.W., Pai, N., Kaplan, L.M., 2014. Role of the microbiome in energy regulation and metabolism. Gastroenterology 146, 1525–1533. https://doi.org/10.1053/j.gastro.2014.02.008

Ridlon, J.M., Kang, D.J., Hylemon, P.B., 2006. Bile salt biotransformations by human intestinal bacteria. J. Lipid Res. 47, 241–259. https://doi.org/10.1194/jlr.R500013-JLR200

Riglar, D.T., Giessen, T.W., Baym, M., Kerns, S.J., Niederhuber, M.J., Bronson, R.T., Kotula, J.W., Gerber, G.K., Way, J.C., Silver, P.A., 2017. Engineered bacteria can function in the mammalian gut long-term as live diagnostics of inflammation. Nat. Biotechnol. 35, 653–658. https://doi.org/10.1038/nbt.3879

Roberfroid, M., Gibson, G.R., Hoyles, L., McCartney, A.L., Rastall, R., Rowland, I., Wolvers, D., Watzl, B., Szajewska, H., Stahl, B., Guarner, F., Respondek, F., Whelan, K., Coxam, V., Davicco, M.J., Léotoing, L., Wittrant, Y., Delzenne, N.M., Cani, P.D., Neyrinck, A.M., Meheust, A., 2010. Prebiotic effects: Metabolic and health benefits. Br. J. Nutr. 104. https://doi. org/10. 1017 / S0007114510003363

Saha, S., Tariq, R., Tosh, P.K., Pardi, D.S., Khanna, S., 2019. Faecal microbiota transplantation for eradicating carriage of multidrug-resistant organisms: a systematic review. Clin. Microbiol. Infect. Off. Publ. Eur. Soc. Clin. Microbiol. Infect. Dis. 25, 958–963. https://doi. org/10.1016/j.cmi.2019.04.006

Salminen, S., Bouley, C., Boutron, M.-C., Cummings, J.H., Franck, A., Gibson, G.R., Isolauri, E., Moreau, M.-C., Roberfroid, M., Rowland, I., 1998. Functional food science and gastrointestinal physiology and function. Br. J. Nutr. 80, S147–S171. https://doi .org/10. 1079/bjn19980108

Sampson, T.R., Debelius, J.W., Thron, T., Janssen, S., Shastri, G.G., Ilhan, Z.E., Challis, C., Schretter, C.E., Rocha, S., Gradinaru, V., Chesselet, M.F., Keshavarzian, A., Shannon, K.M., Krajmalnik-Brown, R., Wittung-Stafshede, P., Knight, R., Mazmanian, S.K., 2016. Gut Microbiota Regulate Motor Deficits and Neuroinflammation in a Model of Parkinson's Disease. Cell 167, 1469-1480.e12. https://doi. org/10.1016/j.cell.2016.11.018

Sanders, M.E., Merenstein, D.J., Ouwehand, A.C., Reid, G., Salminen, S., Cabana, M.D., Paraskevakos, G., Leyer, G., 2016. Probiotic use in at-risk populations. J. Am. Pharm. Assoc. (2003). 56, 680–686. https://doi.org/10.1016/j.japh.2016.07.001

Santoni, M., Piva, F., Conti, A., Santoni, A., Cimadamore, A., Scarpelli, M., Battelli, N., Montironi, R., 2018. Re: Gut Microbiome Influences Efficacy of PD-1-based Immunotherapy Against Epithelial Tumors. Eur. Urol. 74, 521–522. https://doi.org/10.1016/j.eururo.2018.05.033

Scheiman, J., Luber, J.M., Chavkin, T.A., MacDonald, T., Tung, A., Pham, L.D., Wibowo, M.C., Wurth, R.C., Punthambaker, S., Tierney, B.T., Yang, Z., Hattab, M.W., Avila-Pacheco, J., Clish, C.B., Lessard, S., Church, G.M., Kostic, A.D., 2019. Meta-omics analysis of elite athletes identifies a performance-enhancing microbe that functions via lactate metabolism. Nat. Med. 25, 1104–1109. https://doi. org/10.1038/s41591-019-0485-4

Selma, M. V., Espín, J.C., Tomás-Barberán, F.A., 2009. Interaction between phenolics and gut microbiota: Role in human health. J. Agric. Food

Chem. 57, 6485–6501. https://doi.org/10.1021/jf902107d

Sender, R., Fuchs, S., Milo, R., 2016. Revised Estimates for the Number of Human and Bacteria Cells in the Body. PLoS Biol. 14, e1002533. https://doi.org/10.1371/journal.pbio.1002533

Sokol, H., Pigneur, B., Watterlot, L., Lakhdari, O., Bermúdez-Humarán, L.G., Gratadoux, J.-J., Blugeon, S., Bridonneau, C., Furet, J.-P., Corthier, G., Grangette, C., Vasquez, N., Pochart, P., Trugnan, G., Thomas, G., Blottière, H.M., Doré, J., Marteau, P., Seksik, P., Langella, P., 2008. Faecalibacterium prausnitzii is an anti-inflammatory commensal bacterium identified by gut microbiota analysis of Crohn disease patients. Proc. Natl. Acad. Sci. U. S. A. 105, 16731–16736. https://doi.org/10.1073/pnas.0804812105

Sonnenburg, E.D., Sonnenburg, J.L., 2014. Starving our microbial self: The deleterious consequences of a diet deficient in microbiota-accessible carbohydrates. Cell Metab. 20, 779–786. https://doi.org/10.1016/j.cmet.2014.07.003

Tremaroli, V., Bäckhed, F., 2012. Functional interactions between the gut microbiota and host metabolism. Nature 489, 242–249. https://doi.org/10.1038/nature11552

Turnbaugh, P.J., Ley, R.E., Mahowald, M.A., Magrini, V., Mardis, E.R., Gordon, J.I., 2006. An obesity-associated gut microbiome with increased capacity for energy harvest. Nature 444, 1027–1031. https://doi.org/10.1038/nature05414

Vangay, P., Ward, T., Gerber, J.S., Knights, D., 2015. Antibiotics, pediatric dysbiosis, and disease. Cell Host Microbe 17, 553–564. https://doi.org/10.1016/j.chom.2015.04.006

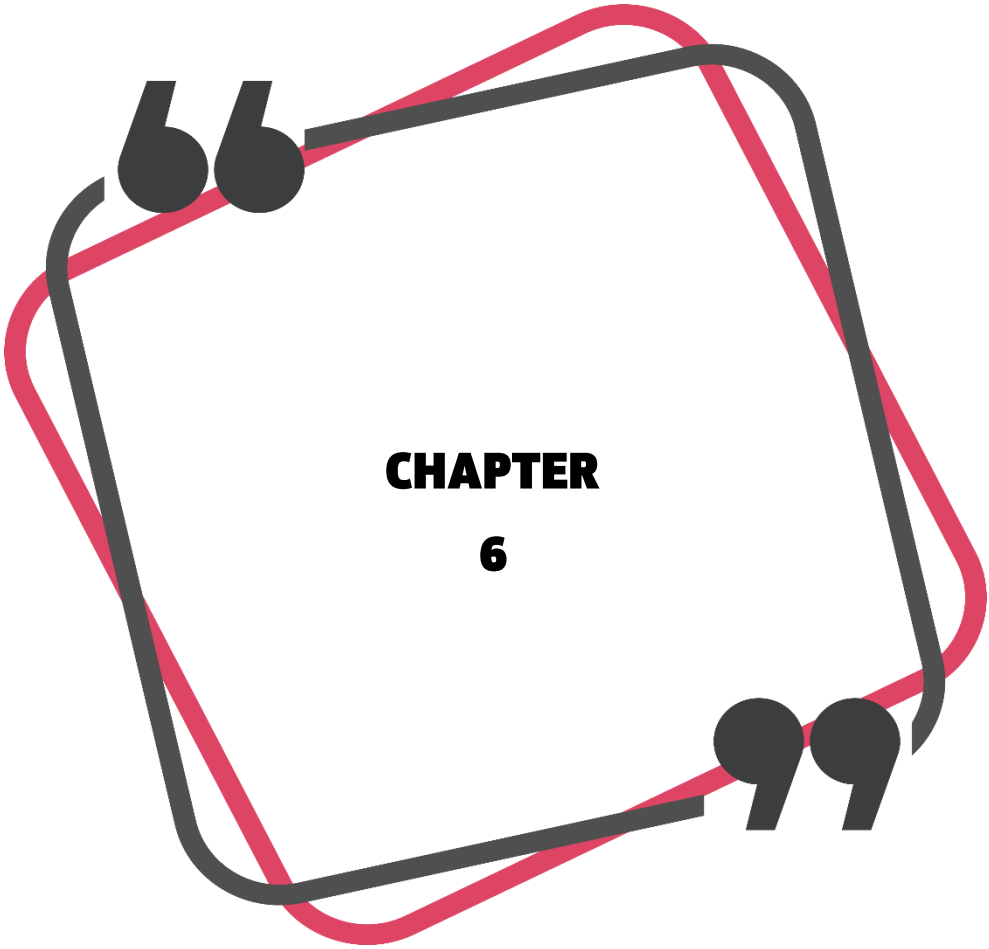
Viaud, S., Daillère, R., Boneca, I.G., Lepage, P., Langella, P., Chamaillard, M., Pittet, M.J., Ghiringhelli, F., Trinchieri, G., Goldszmid, R., Zitvogel, L., 2015. Gut microbiome and anticancer immune response: Really hot Sh∗t! Cell Death Differ. 22, 199–214. https://doi.org/10.1038/cdd.2014.56

Wang, Jun, Qin, J., Li, Y., Cai, Z., Li, Shenghui, Zhu, J., Zhang, F., Liang, S., Zhang, W., Guan, Y., Shen, D., Peng, Y., Zhang, D., Jie, Z., Wu, W., Qin, Y., Xue, W., Li, J., Han, L., Lu, D., Wu, P., Dai, Y., Sun, X., Li, Z., Tang, A., Zhong, S., Li, X., Chen, W., Xu, R., Wang, M., Feng, Q., Gong, M., Yu, J., Zhang, Y., Zhang, M., Hansen, T., Sanchez, G., Raes, J., Falony, G., Okuda, S., Almeida, M., Lechatelier, E., Renault, P., Pons, N., Batto, J.M., Zhang, Z., Chen, H., Yang, R., Zheng, W., Li, Songgang, Yang, H., Ehrlich, S.D., Nielsen, R., Pedersen, O., Kristiansen, K., Wang, Jian, 2012. A metagenome-wide association study of gut microbiota in type 2 diabetes. Nature 490, 55–60.

ISBN: 978-625-6971-51-6

https://doi.org/10.1038/nature11450

Wang, Y., Wiesnoski, D.H., Helmink, B.A., Gopalakrishnan, V., Choi, K., DuPont, H.L., Jiang, Z.-D., Abu-Sbeih, H., Sanchez, C.A., Chang, C.-C., Parra, E.R., Francisco-Cruz, A., Raju, G.S., Stroehlein, J.R., Campbell, M.T., Gao, J., Subudhi, S.K., Maru, D.M., Blando, J.M., Lazar, A.J., Allison, J.P., Sharma, P., Tetzlaff, M.T., Wargo, J.A., Jenq, R.R., 2018. Fecal microbiota transplantation for refractory immune checkpoint inhibitor-associated colitis. Nat. Med. 24, 1804–1808. https://doi.org/10.1038/s41591-018-0238-9


CHAPTER
6

ISBN: 978-625-6971-51-6

FIRST TESS LIGHT CURVE SOLUTION OF V458 AND

Research Asst. Oğuz ÖZTÜRK, PhD

Çanakkale Onsekiz Mart University
Faculty of Science, Department of Physics
Çanakkale Onsekiz Mart University
Astrophysics Research Centre and Observatory
ORCID: 0000-0002-9135-9865

Introduction

There are many binary star systems in the universe. These binary star systems made of two stars orbiting each other. During the orbital motion, both stars pass in front of each other. A periodic variation in the total amount of light coming from the system can be detected by an observer on Earth if the inclination is around ~90 degree. Such binary star systems are called as eclipsing binary star systems.

Absolute parameters, i.e. masses, radii and effective temperatures of the components, can be obtained via spectroscopic and photometric observations. In this way, relationships between these parameters can be investigated and the ages of stars can be estimated (see Demircan & Kahraman 1991, Malkov et al. 2007, Negu & Tessema 2018). As a result of sensitively determined stellar parameters, stellar evolution models can be developed.

Light curve of V458 And obtained from the Transiting Exoplanet Sur-vey Satellite (TESS) (Ricker et al. 2015) observations is examined in this study. In classical Algol-type binary star systems, the one component (primary) star is a hot massive star that does not fill its Roche lobe, while the other component (secondary) is a cold less massive star that fills its Roche lobe (see Kopal 1955, Peters 2001). Therefore, Algol-type binary star systems are classified as semi-detached binary star systems according to their Roche geometry.

Observational Data

The TESS observations are taken from the Mikulski Archive for Space Telescopes database. The light curve was constructed using the SAP_FLUX measurements given in the database. QUALITY = 0 observations, which are specified as

the most sensitive observation points in the database, were used in the solution. TESS observations were made using broad band filters (600 nm to 1000 nm).

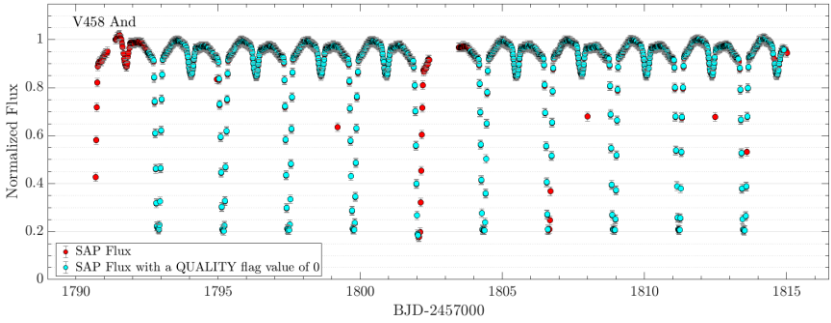


Figure 1. Light curve of V458 And used in this study.

In these observations, different sky regions were observed at different time intervals. In the TESS observations, the "sector" number is given to indicate this situation. For example, TESS observations of V458 And were made in sector 18. Observations made in sector 18 were carried out between 3 November 2019 and 27 November 2019. Exposure time of 1800s is given in the observations of the V458 And. 993 of the observations have a QUALITY flag value of zero. The light curve of V458 And is given in Figure 1.

Table 1. Minimum times of V458 And obtained from TESS observations.

Minimum time (BJD)	**Error**	**Minimum type**
2458791.755505	0.002060	Min II
2458792.889711	0.001060	Min I
2458794.043286	0.001247	Min II
2458795.180340	0.000747	Min I
2458796.332433	0.001426	Min II
2458797.470338	0.000971	Min I
2458798.620724	0.000820	Min II
2458799.761050	0.000865	Min I
2458800.913762	0.001139	Min II

ISBN: 978-625-6971-51-6

2458802.054270	0.001374	Min I
2458804.342024	0.000767	Min I
2458805.495861	0.001453	Min II
2458806.632509	0.000624	Min I
2458807.787925	0.001681	Min II
2458808.923195	0.000851	Min I
2458810.074408	0.001430	Min II
2458811.213477	0.001251	Min I
2458812.369204	0.002202	Min II
2458813.503930	0.000646	Min I
2458814.664870	0.003404	Min II

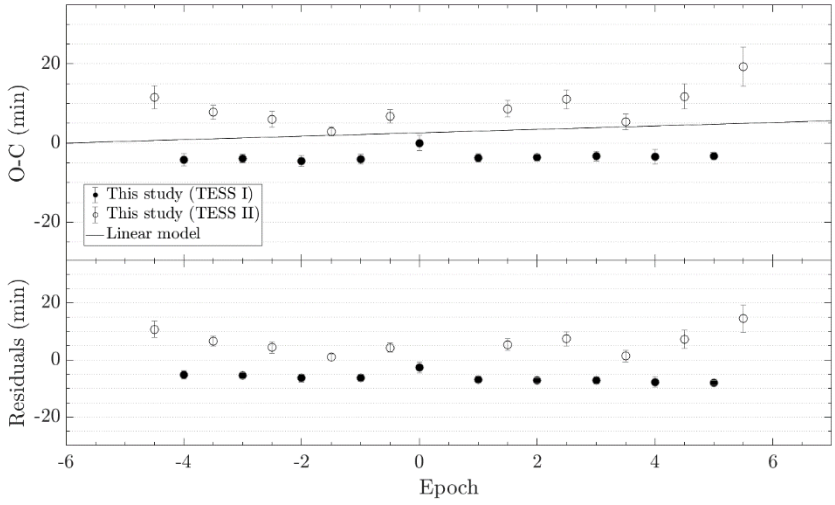


Figure 2. O-C diagram of V458 And obtained from TESS minimum times.

The minimum times (eclipse times) obtained from these observations were calculated using a method proposed by Kwee & van Woerden (1956) (see Table 1).

From the TESS minimum times of V458 And (see Table 1), using the light element below, the O-C diagram was made (see Figure 2).

$$C_{1,\mathrm{V458\ And}}(\mathrm{Min\ I/Min\ II}) = \mathrm{BJD}\ 2458802.05427(137) + 2^{\mathrm{d}}.2902696 \times E \quad (1)$$

In Equation (1), the conjunction time (2458802.05427(137) BJD) is a calculated TESS minimum time (see Table 1) and the period (2.2902696 days) is taken from the ASAS-SN database (Shappee et al. 2014, Kochanek et al. 2017). Using the least squares method, linear fit was made to the diagram and the updated light element of V458 And is derived as follows,

$$C_{2,\mathrm{V458\ And}}(\mathrm{Min\ I/Min\ II}) = \mathrm{BJD}\ 2458802.0561(11) + 2^{\mathrm{d}}.2907(4) \times E \quad (2)$$

The TESS light curve of V458 And phased with Equation (2) is presented in Figure 3.

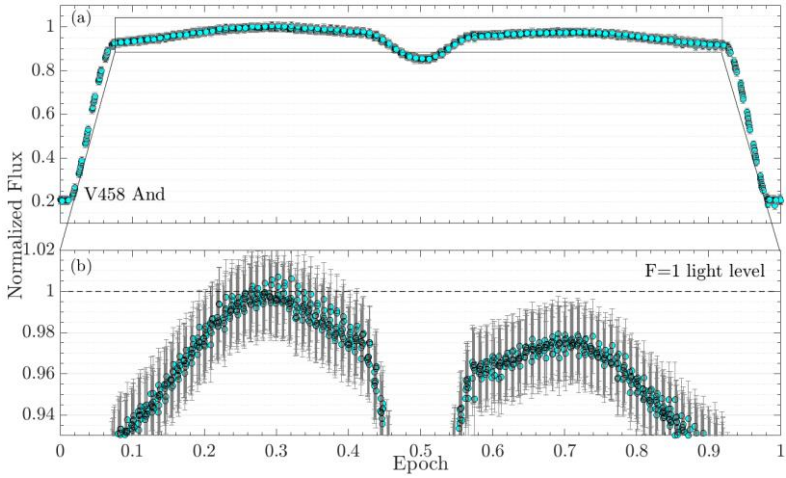


Figure 3. (a) Phased light curve of V458 And (b) Zoom of maximum levels of light curve.

ISBN: 978-625-6971-51-6

Light Curve Solution

Light curve analysis of V458 And was performed using Wilson-Devinney software (Wilson & Devinney, 1971; Wilson, 2012). In the solution, the wavelength of the filter is taken as 786.5nm. According to the radiative (T>7200K) and convective (T<7200) stellar atmospheres, the bolometric gravitational darkening coefficients (g_1 and g_2) were taken as 1.0 and 0.32, respectively (von Zeipel, 1924; Lucy, 1967). The bolometric albedo of the components (A_1 and A_2) is fixed at 1.0 for stellar atmospheres with radiative atmospheres and 0.5 for stellar atmospheres with convective atmospheres (Ruciński, 1969). The second order limb darkening coefficients were taken from Claret (2017). The rotation parameters were taken as $F_1 = F_2 = 0$ and the eccentricity as $e = 0$.

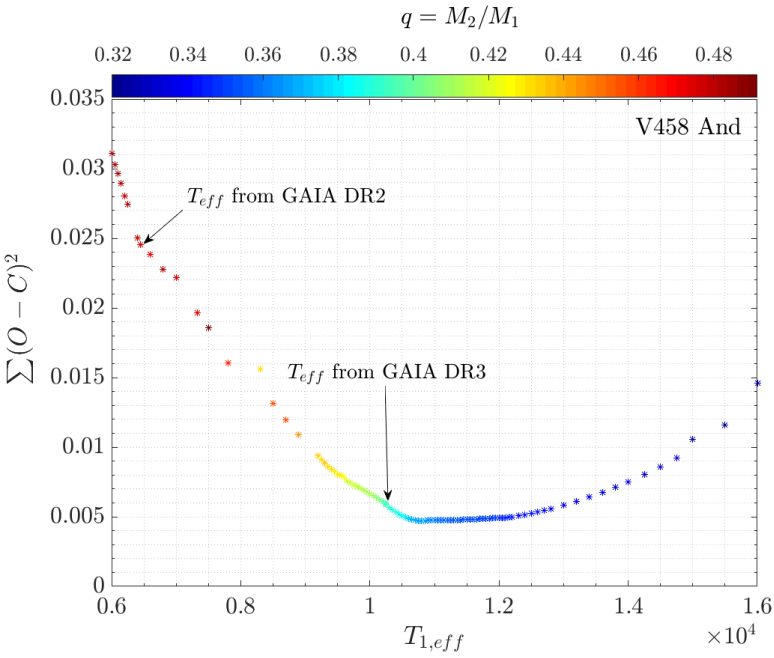


Figure 4. $T_{1,eff}$-$\sum(O-C)^2$ diagram obtained for V458 And under assumption of a cold spot on secondary component.

The solution is done in semi-detached configuration (mod5), where phase shift (ϕ), orbital inclination (i), effective temperature of the secondary component (T_2), surface potential of the primary component (Ω_1), mass ratio (q) and radiation of the primary component (L_1) are free parameters. The third light (L_3) contribution was not included in the solution.

An obvious difference between the maximum light levels can be seen in Figure 3(b). Due to this, the light curve solution was made separately by assuming that there is a hot spot on the primary or a cold spot on the secondary. Therefore, the spot parameters (see Table 2) were also adjusted as free parameters.

The effective temperature of V458 And is given as 6442 K and ~10237K in the Gaia DR2 (Gaia Collaboration, 2018; Andrae et al., 2018) and Gaia DR3 (Gaia Collaboration, 2022) databases, respectively. The error of the temperature values is about 324 K (Gaia Collaboration, 2018; Andrae et al., 2018). As can be seen, the temperature values are given at different values in different databases. In addition to this, there are no spectroscopic observations of the system. Therefore, initially, an effective temperature (T_1) search was made for the primary component of V458 And. In the temperature search process, light curve solution is made for different values of T_1. The variation of T_1 with the sum of squares residuals obtained from the model fit ($\sum(O-C)^2$) is given in Figure 4.

The minimum value of $\sum(O-C)^2$ is obtained under the cold spot assumption. As can be seen in Figure 4, the minimum $\sum(O-C)^2$ value reached at the effective temperature given by Gaia DR3 is smaller than that of the value reached at the effective temperature given by Gaia DR2. Therefore, T_1 is taken form Gaia DR3 and fixed in the light curve solution. As seen from Figure 4, the minimum value of $\sum(O-C)^2$ is also reached around at $q = 0.39$ so that initial value of the q parameter was taken as 0.39 in the analysis.

The obtained light curve parameters are given in Table 2 and the light curve model is shown in Figure 5. The Roche geometry of the system is also shown in Figure 6.

ISBN: 978-625-6971-51-6

Table 2. Parameters obtained from light curve analysis of V458 And.

Parameter	Value
T_0 (BJD)	2458802.0561±0.0011
P (days)	2.2907± 0.0004
ϕ	0.0007±0.0001
i (deg)	85.45±0.21
T_1 (K)	10237
T_2 (K)	4559±135
$q(=M_2/M_1)$	0.394±0.008
Ω_1	6.300±0.007
Ω_2	2.665
r_1 (vol.)	0.170±0.006
r_2 (vol.)	0.331±0.007
L_1/L_{tot}	0.750±0.010
L_2/L_{tot}	0.250
Spot parameters	
Co-latitude (deg.)	104±21
Longitude (deg.)	265±10
Spot radius (deg.)	19.4±1.2
T_{spot}/T_2	0.70±0.05
$\sum(O-C)^2$	0.0060

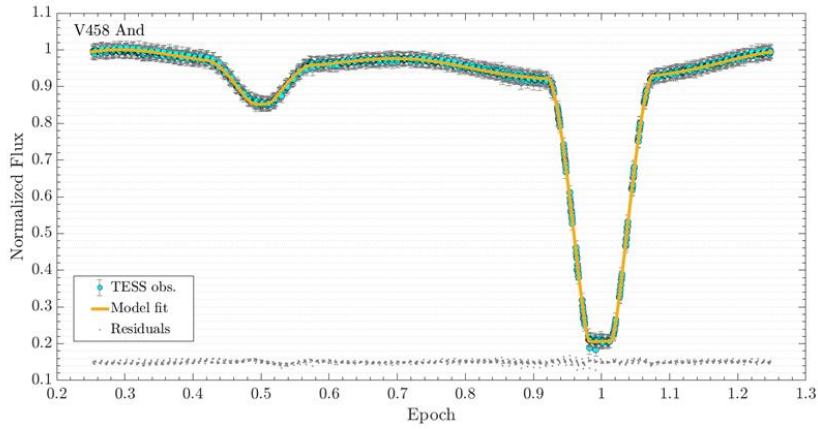
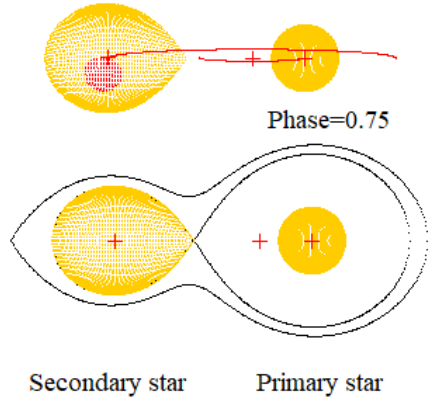


Figure 5. TESS observations of V485 And and best theoretical model fit (yellow line) for these observations. Residuals are shown at bottom.



F**igure 6.** Roche geometry of V458 And.

Results and Discussion

The TESS light curve solution of the V458 And is given for the first time. The absolute parameters estimated using the parameters obtained from the solution are given in Table 5.

ISBN: 978-625-6971-51-6

Table 5. Estimated absolute parameters of V458 And.

Parameter	Primary star	Secondary star
A ($R_\odot$)	11.96±0.24	
M ($M_\odot$)	3.15±0.31	1.24±0.24
R ($R_\odot$)	2.03±0.16	3.96±0.58
$\log g$ (cgs)	4.32±0.10	3.34±0.08
M_{bol} (mag)	0.73±0.10	2.79±0.36
M_V (mag)	1.07±0.25	3.38±0.45
$A_{d,V}$ [(a)] (mag)	0.465	
m_V (system) [(b)] (mag)	13.114±0.274	
M_V (system)	0.95±0.30	
d (pc)	2185±273	

What the parameters given in Table 5 represent and how they were calculated are explained below.

- *Semi-major axis (A):* this parameter was obtained using Kepler's third law, given below.

$$A = \left[\frac{(M_1 + M_2)P^2}{0.01346}\right]^{1/3} \quad (3)$$

From Equation (3), the parameter A is obtained in solar radius, when the stellar masses (M_1 and M_2) are taken in solar mass and orbital period (P) in days.

- *Stellar masses (M_1 and M_2):* M_1 was calculated from the calibrations for the main sequence stars given by Drilling & Landolt's (2000). 10 percent of the primary mass is taken as the error value. On the other hand, M_2 was calculated using the mass ratio ($q = M_2/M_1$) given in Table 2 and the primary mass mentioned above.
- *Stellar radii (R_1 and R_2):* The radii of the component stars that make up V458 And were calculated using the semi-major axis length calculated by Equation (3) together with the fractional radius ($r_{1,2} = R_{1,2}/A$) obtained from the solution.

- *Surface gravities of the components (*$\log g_1$ *and* $\log g_2$*):* The surface gravities were calculated using equation below, where $g_\odot = 27423.2(7.9)$ cm s^{-2} is the surface gravity of Sun (Pecaut & Mamajek (2013)).

$$g_{1,2} = g_\odot \frac{M_{1,2}}{{R_{1,2}}^2} \quad (4)$$

Unit of $M_{1,2}$ and $R_{1,2}$ are in solar mass and solar radius, respectively.

- *Bolometric magnitudes of the components (*$M_{bol,1,2}$*):* Equation given below was used in the calculation of $M_{bol,1,2}$.

$$M_{bol,1,2} = M_{bol,\odot} + 10 \log_{10} \frac{T_{eff,\odot}}{T_{eff,1,2}} - 5 \log_{10} R_{1,2} \quad (5)$$

where $M_{bol,\odot} = 4.7554(4)$ mag, $T_{eff,\odot} = 5771.8(7)$ K are bolometric magnitude and effective temperature of Sun, respectively, and taken from Pecaut & Mamajek (2013).

- *Absolute visual magnitudes (*$M_{V,1,2}$*):* $M_{V,1,2}$ were estimated using equation below, the bolometric corrections ($BC_{V,1,2}$) were calculated using the effective temperature-bolometric correction calibration presented by Pecaut & Mamajek (2013).

$$M_{V,1,2} = M_{bol,1,2} - BC_{V,1,2} \quad (6)$$

- *Interstellar absorption (*$A_{d,V}(b)$*):* An equation given by Bahcall & Soneira (1980) bellow was used to calculate the interstellar absorption, where $b, A_{\infty,V}(b), d$ and H represents the galactic latitude of the system, V band total absorption of the system, the distance and the scale height of the system.

$$A_{d,V}(b) = A_{\infty,V}(b) \left[1 - \exp\left(-\frac{|d \sin b|}{H}\right)\right] \quad (7)$$

$A_{\infty,V}(b)$ was taken from Schlafly & Finkbeiner (2011) (http://ned.ipac.caltech.edu/forms/calculator.html). H was taken to be 125pc according to Marshall et al. (2006).

- *Visual magnitudes (*m_V (system)*):* m_V (system) was taken from the APASS database (Henden et al. 2015).

ISBN: 978-625-6971-51-6

- *Absolute visual magnitude (M_V* (system)*): M_V* (system) of V458 And was estimated using equation below.

$$M_V(\text{system}) = -2.5\log_{10}(10^{-0.4M_{V,1}} + 10^{-0.4M_{V,2}}) \quad (8)$$

- *Distance from us (d):* The distance of the system is calculated from equation below, where the interstellar absorption is also taken into account.

$$d = 10^{\frac{m_V(system) - M_V(system) + 5 - A_{d,V}(b)}{5}} \quad (9)$$

It was concluded that the secondary completely filled its Roche lobe, while the primary did not fill its Roche lobe (see Figure 6). Therefore, a mass transfer from the secondary to the primary can occur. In this case, the orbital period will increase. However, there are currently insufficient numbers of minimum times in the literature to verify the period increase (see O-C gateway, http://var2.astro.cz/ocgate/). To further clarify this situation, in the literature, only 7 minimum times obtained from the observations of this system between 1999 and 2016 are given (see O-C gateway). In addition to the minimum times published so far, in this study 20 minimum times were obtained from the TESS photometric observations made in 2019 (see Table 1). Unfortunately, it is not possible to sensitively examine the orbital period change of this system using all available minimum times. Therefore, sensitive minimum time observations of the system that can be observed in the future are needed to verify the expected orbital period increase.

As mentioned before, the absolute parameters (see Table 5) are estimated using the calibrations available in the literature and the light curve solution parameters obtained in this study. Therefore, the absolute parameter values of the system given here should be supported by future sensitive spectral observations of V458 And.

References

Bahcall, J.N., Soneira, R.M., 1980. The universe at faint magnitudes, I. Models for the Galaxy and the predicted star counts. Astrophys. J. Suppl. 44, 73–110.

Claret, A., 2017, Limb and gravity-darkening coefficients for the TESS satellite at several metallicities, surface gravities, and microturbulent velocities. A&A 600, id.A30.

Demircan, O., Kahraman, G. 1991. Stellar Mass / Luminosity and Mass / Radius Relation. Astrophysics and Space Science, Volume 181, Issue 2, pp.313-322, 181, 313.

Drilling, J.S., Landolt, A.U., 2000. In: Cox, Arthur N. (Ed.), Allen's Astrophysical Quantities, fourth ed. AIP Press; Springer, New York, ISBN: 0-387-98746-0, p. 381.

Gaia Collaboration, 2018, Gaia Data Release 2. Summary of the contents and survey properties. A&A 616, id.A1.

Gaia Collaboration, 2022, VizieR Online Data Catalog: Gaia DR3 Part 1. Main source (Gaia Collaboration, 2022), p. I/355

Henden, A.A., Levine, S., Terrell, D., Welch, D.L., 2015. APASS- The latest data release. In: AAS Meeting #225. 336,16.

Kochanek, C. S., Shappee, B. J., Stanek, K. Z., ve ark. 2017, The All-Sky Automated Survey for Supernovae (ASAS-SN) Light Curve Server v1.0. PASP 129 (980), pp. 104502.

Kopal, Z. 1955. The classification of close binary systems. Annales d'Astrophysique, Vol. 18, p.379.

Kwee, K. K., van Woerden, H., 1956, A method for computing accurately the epoch of minimum of an eclipsing variable. BAN 12,327-330.

Lucy, L. B., 1967, Gravity-Darkening for Stars with Convective Envelopes. ZA 65, 89-92.

Malkov, O. Y., Oblak, E., Avvakumova, E. A., Torra, J. 2007. A procedure for the classification of eclipsing binaries. Astronomy and Astrophysics, Volume 465, Issue 2, April II 2007, pp.549-556.

Marshall, D.J., Robin, A.C., Reyl´e, C., et al., 2006. Modelling the galactic interstellar extinction distribution in three dimensions. AA 453 (2), 635–651.http://dx.doi.org/10.1051/0004-6361:20053842

ISBN: 978-625-6971-51-6

Negu, S. H., Tessema, S. B. 2018. Statistical analysis of Algol-type eclipsing binaries with stable mass transfer. Astronomische Nachrichten, Volume 339, Issue 709, pp. 709-717.

Pecaut, M.J., Mamajek, E.E., 2013. Intrinsic colors, temperatures, and bolometric corrections of pre-main-sequence stars. Astrophys. J. Suppl. 208 (1), 9.

Peters, G. J. 2001. Introduction The Accretion Disk The Gas Stream The High Temperature Accretion Region Domains of Outflow Putting it All Together Concluding Remarks. The influence of binaries on stellar population studies, Dordrecht: Kluwer Academic Publishers, 2001, xix, 582 p. Astrophysics and space science library (ASSL), Vol. 264. ISBN 0792371046, p.79.

Ricker, G.R., Winn, J.N., Vanderspek, R., et al., 2015. Transiting exoplanet Survey satellite (TESS). JATIS 1 (1), 014003.

Ruciński S. M., 1969, The Proximity Effects in Close Binary Systems. II. The Bolometric Reflection Effect for Stars with Deep Convective Envelopes. AcA 19, 245-255

Schlafly, E.F., Finkbeiner, D.P., 2011. Measuring reddening with sloan digital sky Survey stellar spectra and recalibrating SFD. Astrophys. J. 737 (2).

Shappee, B. J., Prieto, J. L., Grupe, D. ve ark. 2014, The Man behind the Curtain: X-Rays Drive the UV through NIR Variability in the 2013 Active Galactic Nucleus Outburst in NGC 2617. ApJ 788 (1), id.48.

von Zeipel, H., 1924. The radiative equilibrium of a rotating system of gaseous masses. MNRAS 84, 665–683.

Wilson, R. E., 2012, Spotted Star Light Curves with Enhanced Precision. AJ 144 (3), id.73.

Wilson, R.E., Devinney, E.J., 1971. Realization of accurate close-binary light curves: Application to MR cygni. Astrophys. J. 166, 605–619.